Available online at www.sciencedirect.com

SciVerse ScienceDirect

Geochimica et Cosmochimica Acta 95 (2012) 15–34

Geochimica et Cosmochimica Acta

www.elsevier.com/locate/gca

# The effect of carbonic anhydrase on the kinetics and equilibrium of the oxygen isotope exchange in the $CO_2$–$H_2O$ system: Implications for $\delta^{18}O$ vital effects in biogenic carbonates

Joji Uchikawa *, Richard E. Zeebe [1]

*Department of Oceanography, SOEST, University of Hawaii at Manoa, 1000 Pope Road, Honolulu, HI 96822, USA*

Received 17 February 2012; accepted in revised form 17 July 2012; available online 1 August 2012

**Abstract**

Interpretations of the primary paleoceanographic information recorded in stable oxygen isotope values ($\delta^{18}O$) of biogenic $CaCO_3$ can be obscured by disequilibrium effects. $CaCO_3$ is often depleted in $^{18}O$ relative to the $\delta^{18}O$ values expected for precipitation in thermodynamic equilibrium with ambient seawater as a result of vital effects. Vital effects in $\delta^{18}O$ have been explained in terms of the influence of fluid pH on the overall $\delta^{18}O$ of the sum of dissolved inorganic carbon (DIC) species (often referred to as "pH model") and in terms of $^{18}O$ depletion as a result of the kinetic effects associated with $CO_2$ hydration ($CO_2 + H_2O \leftrightarrow H_2CO_3 \leftrightarrow HCO_3^- + H^+$) and $CO_2$ hydroxylation ($CO_2 + OH^- \leftrightarrow HCO_3^-$) in the calcification sites (so-called "kinetic model"). This study addresses the potential role of an enzyme, carbonic anhydrase (CA), that catalyzes inter-conversion of $CO_2$ and $HCO_3^-$ in relation to the underlying mechanism of vital effects. We performed quantitative inorganic carbonate precipitation experiments in order to examine the changes in $^{18}O$ equilibration rate as a function of CA concentration. Experiments were performed at pH 8.3 and 8.9. These pH values are comparable to the average surface ocean pH and elevated pH levels observed in the calcification sites of some coral and foraminiferal species, respectively. The rate of uncatalyzed $^{18}O$ exchange in the $CO_2$–$H_2O$ system is governed by the pH-dependent DIC speciation and the kinetic rate constant for $CO_2$ hydration and hydroxylation, which can be summarized by a simple mathematical expression. The results from control experiments (no CA addition) are in agreement with this expression. The results from control experiments also suggest that the most recently published kinetic rate constant for $CO_2$ hydroxylation has been overestimated. When CA is present, the $^{18}O$ equilibration process is greatly enhanced at both pH levels due to the catalysis of $CO_2$ hydration by the enzyme. For example, the time required for $^{18}O$ equilibrium is nearly halved by the presence of $3.7 \times 10^{-9}$ M of CA used for the experiments. Despite its significant influence on the oxygen isotope exchange kinetics, the equilibrium oxygen isotope fractionation between individual DIC species and $H_2O$ is unaffected by CA. Because many $CaCO_3$-secreting organisms possess active CA, our findings imply that $^{18}O$ equilibration of the $CO_2$–$H_2O$ system is possible within realistic timescales of biogenic calcification.


## 1. INTRODUCTION

Stable oxygen isotope values ($\delta^{18}O$) of marine biogenic $CaCO_3$ such as foraminiferal tests and coral skeletons have served as a primary tool to reconstruct past ocean temperatures and global ice volumes on various timescales (e.g., Shackleton and Kennett, 1975; Corrège et al., 2000; Tudhope et al., 2001; Zachos et al., 2001). However, one of the major biases in the paleoceanographic utility of this proxy is that $\delta^{18}O$ values of these carbonates often deviate from the expected thermodynamic equilibrium values as a result of vital effects (Keith and Webber, 1965; McConnaughey, 1989a; Spero et al., 1997; Adkins et al., 2003). Based on the fact that individual dissolved inorganic

* Corresponding author. Tel.: +1 808 956 3285; fax: +1 808 956 7112.

*E-mail addresses:* uchikawa@hawaii.edu (J. Uchikawa), zeebe@soest.hawaii.edu (R.E. Zeebe).

[1] Tel.: +1 808 956 6473; fax: +1 808 956 7112.

0016-7037/$ - see front matter © 2012 Elsevier Ltd. All rights reserved.
http://dx.doi.org/10.1016/j.gca.2012.07.022

carbon (DIC) species have a distinct equilibrium $^{18}O$ fractionation relative to $H_2O$ (McCrea, 1950; Usdowski et al., 1991; Beck et al., 2005), Zeebe (1999) explained such disequilibrium $CaCO_3$ precipitation in terms of the role of fluid pH in defining DIC speciation and therefore the overall $^{18}O$ fractionation between the sum of DIC species and $H_2O$ (see Zeebe, 2007 for revised formulation). Consequently Lea et al. (1999), Zeebe (2001) and Uchikawa and Zeebe (2010) argued that paleotemperature estimates based on foraminiferal $\delta^{18}O$ can be significantly biased for past time intervals when seawater carbonate chemistry was markedly different from modern condition, such as during the last glacial maximum, mid-Cretaceous and Paleocene–Eocene Thermal Maximum.

Another conceptual model attributes the disequilibrium phenomenon to kinetic effects (McConnaughey, 1989a,b, 2003). This model assumes that $CaCO_3$ forms from alkaline fluids in the calcification sites that are isolated by $CO_2$-permeable but $HCO_3^-$-impermeable membranes. Calcification is stimulated by active $Ca^{2+}$ acquisition and simultaneous $H^+$ removal by alkalinity pumps, which establish large pH and $CO_2$ gradients across the membranes. This drives passive diffusion of $CO_2$ into the calcification sites, in which hydration and/or hydroxylation reaction cause strong $^{18}O$-depletion in the resultant $HCO_3^-$. Unless $HCO_3^-$ (and $CO_3^{2-}$) re-equilibrates before calcification, the $^{18}O$-depletion will be recorded in $CaCO_3$. This kinetic model is popularly referred to as a leading explanation for the $^{18}O$ depletion in coral skeletons observed *in situ* and from culture experiments (Allison et al., 1996; Felis et al., 2003; Rosenfeld et al., 2003; Maier et al., 2004; Omata et al., 2008).

More recently an innovative technique for simultaneous $\delta^{18}O$ and $\delta^{11}B$ measurements on μm-scale resolution has been developed with the use of ion microprobes (Rollion-Bard et al., 2003, 2008, 2010, 2011; Juillet-Leclerc et al., 2009). Rollion-Bard et al. (2003, 2011) found μm-scale $\delta^{18}O$ fluctuations exceeding 10‰ for a segment of symbiotic coral skeleton as opposed to only ~2‰ variations resolved by bulk $\delta^{18}O$ measurements on a mm-scale sampling resolution. Their coupled $\delta^{11}B$ analyses also revealed concurrent μm-scale fluctuations, which translate to internal pH variations between 7 and 9. They hence argued that internal pH variations modulate carbonate $\delta^{18}O$ signatures by regulating DIC speciation and the kinetics of the oxygen isotope exchange in the $CO_2$–$H_2O$ system. Furthermore Rollion-Bard et al. (2008, 2010) and Juillet-Leclerc et al. (2009) argued that the early phases of calcification in close association with an organic matrix or certain organic molecules may be crucial for $\delta^{18}O$ heterogeneity in distinct microstructures of foraminiferal tests and coral skeletons. From these findings it appears that the conceptual models based on just inorganic carbonate chemistry are too simplistic to explain intra-test/skeletal $\delta^{18}O$ variability, and thus biochemical perspectives also need to be considered for a realistic explanation of vital effects. One of the key biochemical aspects is the role of enzymes during calcification. For instance, an enzyme Ca-ATPase seems to be crucial in maintaining high pH and $[Ca^{2+}]$ for the extracellular calcification fluid in corals and foraminifera (McConnaughey, 1989b; Ip et al., 1991; Adkins et al., 2003; Erez, 2003). Another potentially important enzyme, which will be explored in this study, is carbonic anhydrase (CA).

CA is a zinc-bearing enzyme that catalyzes inter-conversion of $CO_2$ and $HCO_3^-$ via $CO_2$ hydration and its reverse reaction (Paneth and O'Leary, 1985). Many marine calcifiers are known to possess some forms of CA (Nimer et al., 1994; Miyamoto et al., 1996; Furla et al., 2000; Al-Horani et al., 2003; Rost et al., 2003; Soto et al., 2006; Tambutté et al., 2006; Yu et al., 2006; Moya et al., 2008; Bertucci et al., 2011), although their exclusive roles in relation to calcification as well as other metabolic processes are still controversial. Also, it is important to note that $CO_2$ hydration represents the primary pathway in which direct exchange of oxygen isotopes between DIC species and $H_2O$ takes place (Zeebe and Wolf-Gladrow, 2001). In fact the catalytic role of CA on the oxygen isotope exchange during $CO_2$ hydration was experimentally demonstrated by Silverman (1973). Therefore it is expected that the presence of CA should reduce the time necessary for $^{18}O$ equilibration in the $CO_2$–$H_2O$ system. If this also holds true within the calcification sites, $^{18}O$-depletion due to the kinetic effects can be eliminated and the equilibrium $\delta^{18}O$ values at a given pH can be reestablished before calcification. Obviously, this has important implications for both pH-based (Zeebe, 1999; 2007) and kinetic-based (McConnaughey, 1989a,b; 2003) explanations for $\delta^{18}O$ vital effects. Yet a critical unknown is the effectiveness of CA, which depends on the form and concentration of CA and possibly the pH of the aqueous medium. Furthermore, to the best of our knowledge, it is still untested whether the presence of CA alters the equilibrium oxygen isotope fractionations between DIC species and $H_2O$.

In this paper, we report the results from quantitative inorganic carbonate precipitation experiments. The experiments were performed in time-series over the course of $^{18}O$ equilibration in the $CO_2$–$H_2O$ system with variable CA concentrations. The results from control experiments (no CA addition) are used for validation of the mathematical expression for the uncatalyzed rate of oxygen isotope exchange between DIC and $H_2O$ given in Usdowski et al. (1991). Since the derivation was not addressed in the original publication, we comprehensively derive this expression in Appendix A. The results from control experiments also allow assessment of the reliability of the kinetic rate constants for $CO_2$ hydroxylation. Finally, the results from CA experiments are used to evaluate the effect of CA concentration on the kinetics and equilibrium of the oxygen isotope exchange in the $CO_2$–$H_2O$ system. Our experimental results are discussed in the context of $\delta^{18}O$ vital effects.

## 2. UNCATALYZED OXYGEN ISOTOPE EXCHANGE KINETICS IN THE $CO_2$–$H_2O$ SYSTEM

Unfortunately, the derivation of the mathematical expression for the uncatalyzed rate of $^{18}O$ exchange in the $CO_2$–$H_2O$ system in Usdowski et al. (1991) was not described in the original publication. This may hinder the utility of this expression, which can be very useful for a variety of applications. We derive this expression following the

classical work of Mills and Urey (1940), which is summarized in Appendix A.

Dissolved $CO_2$ plays a critical role in $^{18}O$ equilibration because direct exchange of oxygen isotopes between DIC and $H_2O$ is only possible via the $CO_2$ hydration and $CO_2$ hydroxylation reaction (e.g., Zeebe and Wolf-Gladrow, 2001):

$$CO_2 + H_2O \underset{k_{-2}}{\overset{k_{+2}}{\rightleftarrows}} H_2CO_3 \tag{1}$$

and

$$CO_2 + OH^- \underset{k_{-4}}{\overset{k_{+4}}{\rightleftarrows}} HCO_3^- \tag{2}$$

Hence the rate of uncatalyzed oxygen isotope exchange is essentially governed by the kinetic rate constants for the $CO_2$ hydration ($k_{+2}$ and $k_{-2}$) and hydroxylation ($k_{+4}$ and $k_{-4}$) as well as the DIC speciation, which is a function of pH. An equation by Usdowski et al. (1991) describes this relationship (see also Zeebe and Wolf-Gladrow, 2001):

$$\ln\left(\frac{^{18}R_S - {}^{18}R_S^{EQ}}{^{18}R_S^0 - {}^{18}R_S^{EQ}}\right) = -\left(\frac{1}{\tau}\right)\cdot t \tag{3}$$

where $^{18}R_S$, $^{18}R_S^0$, and $^{18}R_S^{EQ}$ represent the oxygen isotope ratio ($^{18}O/^{16}O$) of $S$ at time $t$, $t = 0$, and at equilibrium. Here, $S$ refers to:

$$S = [H_2CO_3] + [HCO_3^-] + [CO_3^{2-}] \tag{4}$$

The inverse time constant $1/\tau$ in (Eq. (3)) is given by:

$$\tau^{-1} = (0.5)\cdot\{k_{+2} + k_{+4}[OH^-]\} \cdot \left\{1 + \frac{[CO_2]}{S} - \left[1 + \left(\frac{2}{3}\cdot\frac{[CO_2]}{S}\right) + \left(\frac{[CO_2]}{S}\right)^2\right]^{1/2}\right\} \tag{5}$$

$[OH^-]$ can be constrained by pH and $K_W$, the equilibrium $H_2O$ dissociation constant. Furthermore, by re-arranging (Eq. (3)), the time required for 99% $^{18}O$ equilibration (denoted as $t_{99\%}$) can be calculated (Zeebe and Wolf-Gladrow, 2001):

$$t_{99\%} = -\ln(0.01)\cdot\tau \tag{6}$$

The ratio $[CO_2]/S$ in (Eq. (5)) at a given pH can be calculated from a set of equilibrium constants summarized in Table 1:

$$\frac{[CO_2]}{S} = [K' + \frac{K'\cdot K_{H_2CO_3}}{[H^+]} + \frac{K'\cdot K_{H_2CO_3}\cdot K''}{[H^+]^2}]^{-1} \tag{7}$$

Because of our experimental conditions, we used freshwater kinetic and equilibrium constants to model the $^{18}O$ exchange kinetics (Table 1). Modeling results with seawater constants can be found in Zeebe and Wolf-Gladrow (2001) and Rollion-Bard et al. (2011).

As shown in Table 1, Usdowski et al. (1991) and Zeebe and Wolf-Gladrow (2001) used the $k_{+4}$ by Pinsent et al. (1956) for their calculations. But we note that recently Wang et al. (2010) reevaluated the temperature dependency of $k_{+4}$. The Arrhenius fitting of their new $k_{+4}$ data against experimental temperatures gives the following relationship:

$$\ln(k_{+4}) = 35.2319 - (7697.3961/T) \tag{8}$$

where $T$ is temperature in Kelvin. Since the new $k_{+4}$ values are greater than previously published data by a factor of about 2, the selection of the numeric value for $k_{+4}$ by Wang et al. (2010) or by Pinsent et al. (1956) results in a notable offset in the calculation for pH > 8, where $CO_2$ hydroxylation becomes comparatively more important (Fig. 1). This topic will be further discussed below.

## 3. METHODS

### 3.1. Brief overview of the experimental approach

The influence of CA on the kinetics and equilibrium of the oxygen isotope exchange in the $CO_2$–$H_2O$ system was investigated by quantitative inorganic carbonate precipitation experiments. When a carbonate mineral is quantitatively precipitated from a $HCO_3^-$ and/or $CO_3^{2-}$ dominated solution (i.e., $HCO_3^-$ and $CO_3^{2-}$ are quasi-instantaneously and completely transformed into the mineral), the $\delta^{18}O$ value of the resultant mineral reflects the weighted average of the oxygen present in $HCO_3^-$ and $CO_3^{2-}$ at the time of precipitation and hence records the

Table 1
A list of the equilibrium constants and kinetic rate constants used for calculation of the ratio $[CO_2]/S$ (see Eqs. (3) and (7)). These freshwater constants were originally compiled by Usdowski et al. (1991).

| Parameter | Chemical reaction | Temperature dependency | Temp. Range (°C) | Reference |
|---|---|---|---|---|
| $K_W$ | $H^+ + OH^- \leftrightarrow H_2O$ | $\log_{10}(K_W) = -(6013.79/T) - 23.6521\cdot\log_{10}(T) + 64.7013$ | 0–60 | Harned and Owen (1958) |
| $k_{+2}$ | $CO_2 + H_2O \rightarrow H_2CO_3$ | $\log_{10}(k_{+2}) = 329.850 - 110.541\cdot\log_{10}(T) - (17265.4/T)$ | 0–38 | Pinsent et al. (1956) |
| $k_{-2}$ | $H_2CO_3 \rightarrow CO_2 + H_2O$ | $\ln(k_{-2}) = -(8417.6955/T) + 31.5294$ | 0–37 | Roughton (1941) |
| $K'$ | $CO_2 + H_2O \leftrightarrow H_2CO_3$ | N/A[†] | | N/A |
| $k_{+4}$ | $CO_2 + OH^- \rightarrow HCO_3^-$ | $\log_{10}(k_{+4}) = 13.635 - (2895/T)$ | 0–40 | Pinsent et al. (1956) |
| $K''$ | $HCO_3^- \leftrightarrow H^+ + CO_3^{2-}$ | $\log_{10}(K'') = -(2902.39/T) + 6.4980 - (0.02379/T)$ | 0–50 | Harned and Scholes (1941) |
| $K_{H_2CO_3}{}^*$ | $H_2CO_3^* \leftrightarrow H^+ + HCO_3^-$ | $\log_{10}(K^*_{H_2CO_3}) = -(3404.71/T) + 14.8435 - 0.032786\cdot T$ | 0–50 | Harned and Davis (1943) |
| $K_{H_2CO_3}$ | $H_2CO_3 \leftrightarrow H^+ + HCO_3^-$ | N/A[‡] | | N/A |

*Remarks:*
$H_2CO_3$ refers to the true carbonic acid, $H_2CO_3$. On the other hand, $H_2CO_3^*$ is defined as $H_2CO_3^* = CO_{2(aq)} + H_2CO_3$.
T refers to the temperature in Kelvin.
[†]The equilibrium constant $K'$ can be calculated as $K' = k_{+2}/k_{-2}$.
[‡]The equilibrium constant $K_{H_2CO_3}$ can be calculated as $K_{H_2CO_3} = K_{H_2CO_3}{}^* \times \{1 + (1/K')\}$.

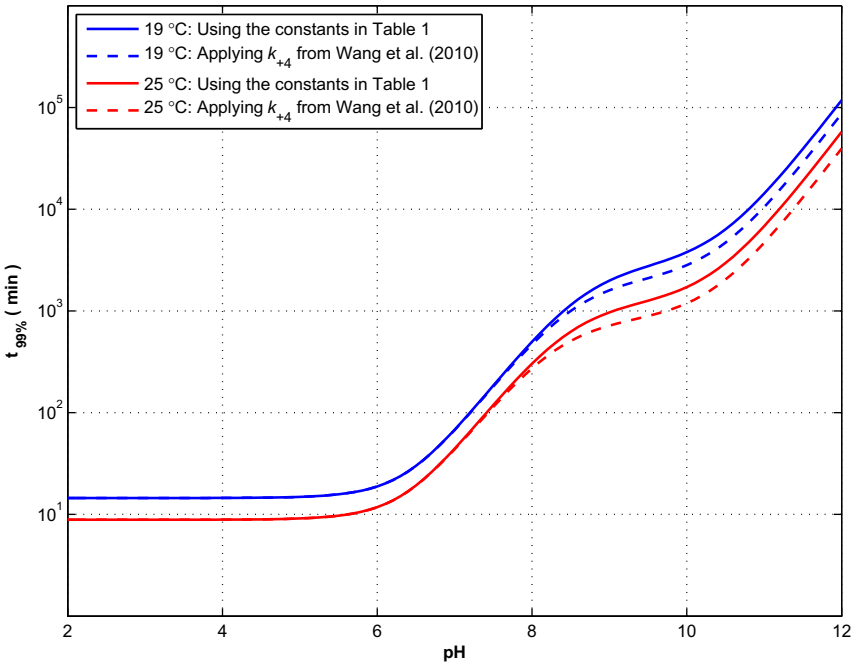


Fig. 1. The time required for 99% completion of uncatalyzed $^{18}O$ equilibration in the $CO_2$–$H_2O$ system ($t_{99\%}$, Eqs. (3) and (6)) as a function of pH. Calculations were made at 0 salinity. (Solid blue) Calculation by Zeebe and Wolf-Gladrow (2001) at 19 °C using the constants in Table 1. (Dashed blue) Calculation at 19 °C using the kinetic constant for $CO_2$ hydroxylation, $k_{+4}$, by Wang et al. (2010). (Solid red) Calculation at 25 °C using the constants listed in Table 1. (Dashed red) Calculation at 25 °C using the $k_{+4}$ by Wang et al. (2010). (For interpretation of the references to colour in this figure legend, the reader is referred to the web version of this article.)

$\delta^{18}O$ of the sum of DIC species (McCrea, 1950; Usdowski et al., 1991; Usdowski and Hoefs, 1993; Zeebe, 1999; Beck et al., 2005). To examine the effect of CA on the kinetics of the oxygen isotope exchange in the $CO_2$–$H_2O$ system and on the equilibrium $^{18}O$ fractionations between DIC species and $H_2O$, quantitative precipitation experiments were conducted as a time-series. Parent $NaHCO_3$ solutions with different CA concentrations were quantitatively transformed into $BaCO_3$ at various times over the course of $^{18}O$ equilibration in the $CO_2$–$H_2O$ by reacting with $BaCl_2{\cdot}2H_2O$ and concentrated NaOH solution. "Time 0" in our experiments refers to the moment when the $NaHCO_3$ powder was dissolved in $H_2O$. The parent $NaHCO_3$ solutions were adjusted to pH 8.3 and pH 8.9. The first value is similar to the average surface ocean pH today and the latter value is particularly relevant to the elevated pH levels within the calcification sites of certain coral and planktonic as well as benthic foraminiferal species (Jørgensen et al., 1985; Rink et al., 1998; Al-Horani et al., 2003; Rollion-Bard et al., 2003; Köhler-Rink and Kühl, 2005; Bentov et al., 2009; de Nooijer et al., 2009; Rollion-Bard and Erez, 2010). Combinations of the CA concentrations and the pH of the parent $NaHCO_3$ solutions tested in our experiments are summarized in Table 2.

### 3.2. Experimental procedures

#### 3.2.1. Preparation and equilibration

Experimental procedures were modified from Beck et al. (2005). The $NaHCO_3$ solutions (0.015 M) were prepared in serum bottles capped and sealed with rubber stoppers and aluminum crimps. Care was taken to minimize the headspace in the bottles. Although the $NaHCO_3$ powder (Certified A.C.S. grade: Fisher Lot #050282) used for the experiments were not isotopically labeled, its $\delta^{13}C$ and $\delta^{18}O$ values were homogeneous ($\delta^{13}C_{VPDB} = -2.89 \pm 0.02‰$, $\delta^{18}O_{VPDB} = -15.81 \pm 0.10‰$, $n = 13$). For the experiments at pH 8.9, the pH of the $NaHCO_3$ solutions was adjusted with 0.5 M NaOH solution prepared from low-carbonate NaOH pellets (Reagent A.C.S. grade: J.T. Baker #3722). Small amounts of CA solutions (see below) were also added to the $NaHCO_3$ solutions for desired concentrations as described in Table 2. All of the solutions described above were prepared using $CO_2$-free deionized $H_2O$. The water was continuously bubbled with $N_2$ gas for a minimum of a week in a large carboy prior to use in order to eliminate dissolved $CO_2$. Aliquots of $H_2O$ used to prepare the $NaHCO_3$ solutions were sampled for $\delta^{18}O$ measurements. The $NaHCO_3$ solutions were equilibrated in water baths maintained at $25 \pm 0.04$ °C using immersion circulators (Thermo Scientific HAAKE C10 and SC100 model).

#### 3.2.2. Quantitative precipitation

The $NaHCO_3$ solutions were withdrawn from the serum bottles and transferred into serum vials containing excess $BaCl_2{\cdot}2H_2O$ powder (Reagent grade: J.T. Baker #0974) under $N_2$-atmosphere. Addition of the $NaHCO_3$ solution resulted in complete dissolution of the $BaCl_2{\cdot}2H_2O$ powder within a few seconds. This step was immediately followed by addition of small amounts of 2.5 M NaOH solution to trigger instantaneous $BaCO_3$ precipitation. Disposable clinical syringes were used for the transfer of the solutions.

Table 2
A summary of the solution chemistry for individual experimental series. All experiments were conducted at 25 °C.

| Experimental series | $NaHCO_3$ conc. (M: mol/L) | pH | CA conc. (mg/mL) | CA conc.[†] (M: mol/L) | Total CA activity (E.U[‡]) |
|---|---|---|---|---|---|
| TS1 (Control) | 0.015 | $8.33 \pm 0.01$ ($n = 15$) | 0 | 0 | 0 |
| TS1-1CA | 0.015 | $8.33 \pm 0.02$ ($n = 15$) | $2.8 \times 10^{-5}$ | $9.3 \times 10^{-10}$ | 2.4 |
| TS1-2CA | 0.015 | $8.34 \pm 0.01$ ($n = 13$) | $5.6 \times 10^{-5}$ | $1.9 \times 10^{-9}$ | 4.7 |
| TS1-intCA | 0.015 | $8.33 \pm 0.01$ ($n = 13$) | $1.1 \times 10^{-4}$ | $3.7 \times 10^{-9}$ | 9.4 |
| TS1-4CA | 0.015 | $8.34 \pm 0.02$ ($n = 13$) | $1.4 \times 10^{-4}$ | $4.6 \times 10^{-9}$ | 11.8 |
| TS1-5CA | 0.015 | $8.34 \pm 0.01$ ($n = 13$) | $2.8 \times 10^{-4}$ | $9.3 \times 10^{-9}$ | 23.6 |
| TS1-6CA | 0.015 | $8.36 \pm 0.02$ ($n = 13$) | $5.6 \times 10^{-4}$ | $1.9 \times 10^{-8}$ | 47.2 |
| TS2 (Control) | 0.015 | $8.89 \pm 0.02$ ($n = 18$) | 0 | 0 | 0 |
| TS2-mnCA | 0.015 | $8.90 \pm 0.02$ ($n = 18$) | $1.1 \times 10^{-4}$ | $3.7 \times 10^{-9}$ | 9.4 |
| TS2-1CA | 0.015 | $8.90 \pm 0.01$ ($n = 22$) | $1.4 \times 10^{-4}$ | $4.6 \times 10^{-9}$ | 11.8 |
| TS2-2CA | 0.015 | $8.90 \pm 0.02$ ($n = 22$) | $2.8 \times 10^{-4}$ | $9.3 \times 10^{-9}$ | 23.6 |
| TS2-3CA | 0.015 | $8.91 \pm 0.03$ ($n = 19$) | $5.6 \times 10^{-4}$ | $1.9 \times 10^{-8}$ | 47.2 |

[†] Molarity (mol/L) was calculated from the molecular weight of the CA reported by the manufacturer (30,000 g/mol).
[‡] Wilbur and Anderson (1948) enzyme unit. The Wilbur–Anderson enzyme unit (E.U) is defined as $E.U = (t_{Blank} - t_{CA})/t_{CA}$ (Eq. (9)).

The precipitates were quickly vacuum-filtered onto 0.2 μm cellulose–nitrate membrane filters and thoroughly rinsed with $CO_2$-free deionized $H_2O$. The $BaCO_3$ samples were oven dried at 65 °C overnight, weighed and stored in air-tight glass vials until stable isotope analyses. For each $NaHCO_3$ solution, quantitative precipitation was performed in duplicate. The remainders of the $NaHCO_3$ solutions were used for pH measurements. We used either a benchtop pH meter (Thermo Scientific Orion 3-Star Plus model) or the auto-titrator system of Zeebe and Sanyal (2002) for the measurements. These instruments were equipped with an Orion triode combination pH electrode (Thermo Scientific #9157BNMD) and an Orion sure-flow pH electrode (Thermo Scientific #8272BN), respectively. The electrodes were calibrated daily using Orion pH buffers (pH 4.01, 7.00, 10.01) that are traceable to NIST standard reference materials.

Precipitation of $BaCO_3$ was selected over $CaCO_3$ in our experiments. This is because $BaCO_3$ only forms a single crystal structure with orthorhombic orientation (as witherite) unlike $CaCO_3$, which can form different types of polymorphs (see Mackenzie and Lerman, 2006). During the method development, our test samples precipitated as $CaCO_3$ indeed resulted in co-precipitation of calcite and variable amounts of vaterite (roughly from 30 to 50% of total $CaCO_3$). Precipitation of a single crystal form is crucial for accurate $\delta^{18}O$ measurements based on the conventional $H_3PO_4$ digestion approach, as described in Kim et al. (2007). X-ray diffraction analyses on select samples confirmed that the precipitated minerals are witherite, regardless of the CA concentration in the parent $NaHCO_3$ solutions.

### 3.3. CA assay

The CA used in this study is of bovine erythrocyte origin. The enzyme was purchased from MP Biomedicals (#153879). Molecular weight of the product reported by the manufacturer is 30,000 g/mol, which is consistent with a published value of $31,000 \pm 1000$ g/mol for bovine erythrocyte CA by Lindskog (1960). The protocols for CA assay for activity measurements were modified from Worthington (1993), which is based on the electrometric approach originally developed by Wilbur and Anderson (1948). A round-bottom flask containing 12 mL of ice-cold 0.02 M Tris–HCl buffer was buried in crushed ice. After thermal equilibration, the reaction was initiated by adding 8 mL of ice-cold $CO_2$ saturated deionized $H_2O$ while gently stirred and the time interval required for the pH decline from 8.3 to 6.3 was measured. The activity was reported in Wilbur–Anderson enzyme unit (E.U) per mg of CA used for assays (Wilbur and Anderson, 1948). The E.U is defined as:

$$E.U = \{(t_{Blank} - t_{CA})/t_{CA}\} \quad (9)$$

where $t_{CA}$ and $t_{Blank}$ are the measured time interval for the pH decline with and without CA in the medium, respectively. For CA assays, 0.04 mL of 0.1 mg/mL CA solution was added to the Tris–HCl buffer. The pH changes during the assay were recorded by the auto-titrator system of Zeebe and Sanyal (2002) described above.

Concentrations of the CA solutions used for the experiments were 0.1 mg/mL and 0.01 mg/mL. These solutions were left at room temperature. Earlier studies demonstrate notable instability of CA and gradual loss of its activity in dilute solutions (e.g., Clark and Perrin, 1951; Thode et al., 1965). As a stability test, we performed daily assays on these CA solutions for 5 consecutive days. No evidence of weakening of the catalytic ability in these CA solutions was observed for the duration (see Section 4.1). Nonetheless, we limited the use of these CA solutions for the experiments within 3 days after preparation in order to ensure the integrity of the CA solutions. After 3 days the CA solutions were discarded and a new solution was freshly prepared. Each experiment series shown in Table 2 were completed within 3 days. In other words, individual $NaHCO_3$ solutions for a given experimental series were prepared from the same CA solution.

### 3.4. Stable isotope analyses

The $BaCO_3$ and $H_2O$ samples were analyzed at University of California Santa Cruz (UCSC) or University of California Davis (UCD) stable isotope laboratory for $\delta^{18}O$ and

$\delta^{13}C$ measurements depending on the instrument accessibility for the analyses at both institutions.

Isotopic analyses of the $BaCO_3$ samples were conducted by the conventional acid digestion approach where samples were reacted with supersaturated $H_3PO_4$ (specific gravity = 1.93 g/cm$^3$) to liberate $CO_2$ gas. At UCSC, ThermoFisher Mat 253 dual-inlet isotope ratio mass spectrometer (IRMS) interfaced to a Kiel IV carbonate device was used. Samples were reacted with $H_3PO_4$ at 75 °C. An in-house working standard and NBS-19 standard were used during the analyses for a drift correction and for the monitoring of the operating condition. Typical precisions were better than ±0.07‰ for $\delta^{18}O$ and ±0.05‰ for $\delta^{13}C$ (±1$\sigma$). At UCD, the $BaCO_3$ samples were digested at 90 °C using an ISOCARB common acid bath autocarbonate device. The resultant $CO_2$ gas was analyzed by a Micromass Optima IRMS. Instrument precisions for carbonate $\delta^{18}O$ and $\delta^{13}C$ analyses based on repeat analyses of an in-house standard were ±0.05‰ and ±0.04‰ (±1$\sigma$), respectively.

The $\delta^{18}O$ values of the $H_2O$ samples were determined by the conventional $CO_2$ equilibration technique. At UCSC, a ThermoFinnigan Delta Plus XP IRMS interfaced to a GasBench II device in continuous flow mode was used. Typical precision from replicate analyses of an in-house standard was better than ±0.07‰. At UCD, an automated equilibrator attached to a Finnigan MAT 251 IRMS was used for the analyses. The analytical precision was better than ±0.03‰.

The isotopic results are reported in $\delta$ notation:

$$\delta = \left(\frac{R_{Sample}}{R_{Standard}} - 1\right) \times 1000 \quad (10)$$

where R is isotope ratio $^{18}O/^{16}O$ or $^{13}C/^{12}C$. The carbonate $\delta^{18}O$ and $\delta^{13}C$ data are reported relative to the VPDB standard, whereas the water $\delta^{18}O$ data are relative to the VSMOW standard. To calculate the isotope fractionation factor between $BaCO_3$ and $H_2O$, the $\delta^{18}O$ values of the $BaCO_3$ samples are also re-scaled to VSMOW following the expression by Coplen et al. (1983):

$$\delta^{18}O_{VSMOW} = 1.0391 \times \delta^{18}O_{VPDB} + 30.91‰ \quad (11)$$

The oxygen isotope fractionation factor $\alpha$ between $BaCO_3$ and $H_2O$ is defined as:

$$\alpha_{BaCO_3-H_2O} = \frac{^{18}R_{BaCO_3}}{^{18}R_{H_2O}} = \frac{\delta^{18}O_{BaCO_3} + 1000}{^{18}O_{H_2O} + 1000} \quad (12)$$

## 4. RESULTS

### 4.1. CA assay and stability test

Based on 6 runs of blanks and CA assays (Fig. 2), $t_{Blank}$ and $t_{CA}$ were 156.8 ± 3.0 and 27.4 ± 1.8 s, respectively. Since $4 \times 10^{-3}$ mg of CA was used for CA assays, the specific activity of the CA used for this study is calculated to be 1179.4 E.U per mg of CA.

As a stability test, we performed daily assays using 0.1 mg/mL and 0.01 mg/mL CA solutions left at room temperatures for 5 consecutive days. Significant slowdown of the pH decline from 8.3 to 6.3 can be considered as the evidence for a weakening of the catalytic ability. Such trend was not observed for the duration of the stability test (Fig. 3). This suggests that both 0.1 mg/mL and 0.01 mg/

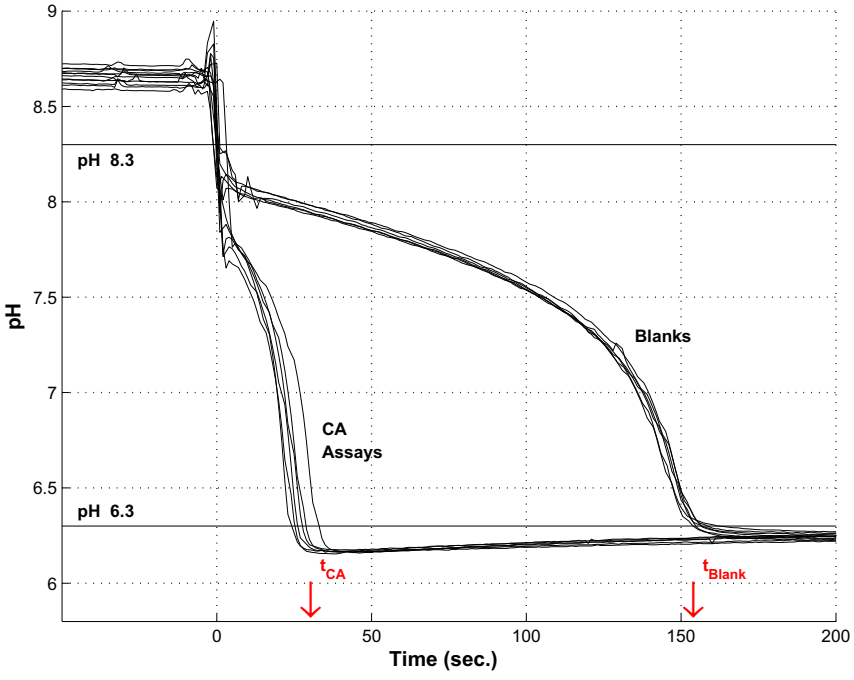


Fig. 2. Determination of the CA activity based on 6 replicate blanks (buffer only) and assays (buffer + CA). The substrate ($CO_2$-saturated $H_2O$) was added to the medium after 3 min of thermal equilibration. The time course of pH decline from 8.3 to 6.3 was recorded to determine $t_{Blank}$ and $t_{CA}$ (Eq. (9)).

mL CA solutions retained their original catalytic ability for well beyond 3 days without refrigeration.

### 4.2. $BaCO_3$ data

The data from quantitative $BaCO_3$ precipitation experiments are presented in the supplementary data (Tables S1–S12). See Appendix B for the online access of the supplementary data.

#### 4.2.1. Data screening

For the purpose of this study, a fundamental requirement is that the $BaCO_3$ samples were indeed *quantitatively* precipitated from the parent $NaHCO_3$ solutions. We assigned two criteria to evaluate the validity of the $BaCO_3$ samples. The first is sample yield in % relative to the theoretical yield, which can be obtained by stoichiometric calculations using the concentration and the volume of the parent $NaHCO_3$ solution used for precipitation. The average yield is $99.4 \pm 1.2\%$ ($n = 380$) when 3 samples with yield below 95% are ignored. The lower yields associated with these 3 samples are all due to mishandling during the filtration and not necessarily reflect incomplete $BaCO_3$ precipitation. The second and more important criterion is the $\delta^{13}C$ values of the $BaCO_3$ samples. Because the $NaHCO_3$ powder used to prepare the parent solutions represents the only carbon source for $BaCO_3$, the $\delta^{13}C$ values of the $NaHCO_3$ ($\delta^{13}C_{VPDB} = -2.89 \pm 0.02‰$, $n = 13$) and $BaCO_3$ samples should be identical if the samples are quantitatively precipitated. Significant offset in the $\delta^{13}C$ values would indicate (1) contamination by absorption of atmospheric $CO_2$ during the solution transfers and/or filtration, (2) incomplete removal of dissolved $CO_2$ in the deionized $H_2O$ used for preparation of various solutions for the experiments, (3) incomplete $BaCO_3$ precipitation or (4) any combinations of the above. The isotopic data for samples whose $\delta^{13}C$ values deviate from that of the source $NaHCO_3$ by more than $\pm 0.5‰$ were rejected for further interpretations. After removing these particular samples (8 samples in total), the $\delta^{13}C$ values of the remaining $BaCO_3$ samples range from $-3.46‰$ to $-2.60‰$ with an average of $-3.19 \pm 0.11‰$ ($n = 375$). Note that the data from 3 particular samples with yields below 95% due to mishandling during filtration mentioned above were not rejected because their $\delta^{13}C$ values are within the $\pm 0.5‰$ threshold. In total 375 samples were considered to be successfully precipitated quantitatively based on both stoichiometric and $\delta^{13}C$ constraints. Accordingly, the $\delta^{18}O_{BaCO_3}$ values obtained from these $BaCO_3$ samples should reflect the overall $\delta^{18}O$ values of the sum of DIC species at the time of precipitation (e.g., Zeebe, 1999; 2007).

#### 4.2.2. Control experiments

Fig. 4 displays the time evolution of the $\alpha_{BaCO_3-H_2O}$ values obtained from TS1 and TS2 control experimental series, where no CA was added to the parent $NaHCO_3$ solutions. Note that well-defined plateaus in the profile indicate $^{18}O$ equilibrium in the $CO_2$–$H_2O$ system. For TS1 control series (average pH of 8.3) the system reaches isotopic equilibrium sometime between 500 and 600 min. In case of TS2 control series (average pH of 8.9), $^{18}O$ equilibration was complete around 1080 min (18 h). Theoretical calculations using the set of constants listed in Table 1 suggest that the $CO_2$–$H_2O$ system comes to 99% completion of $^{18}O$ equilibrium ($t_{99\%}$) in roughly 500 min at pH 8.3 and 900 min at pH 8.9 at 25 °C.

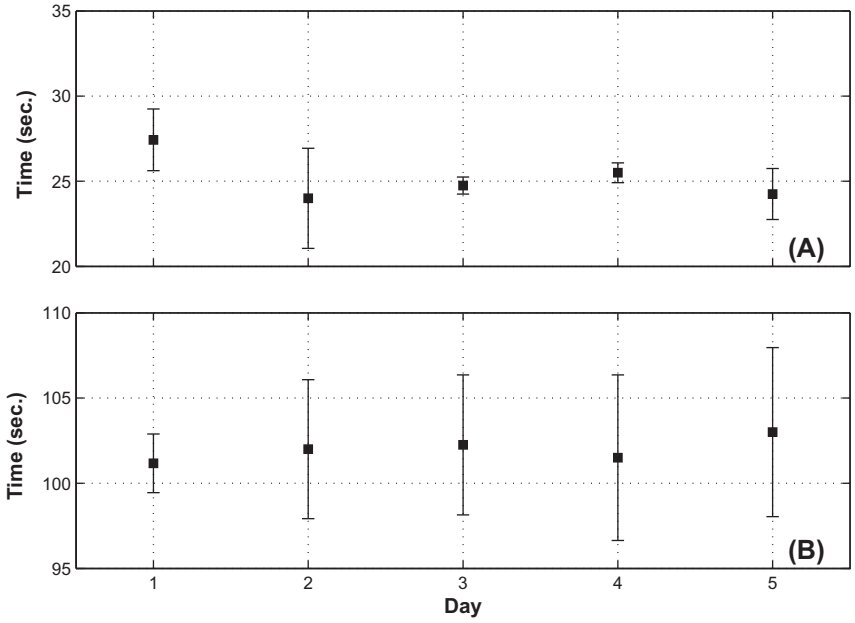


Fig. 3. Stability test for 0.1 mg/mL (Panel A) and 0.01 mg/mL CA solutions (Panel B). Both CA solutions were kept at room temperatures for the duration. Daily results are based on 4 repeated assays, except for the first day when 6 assays were performed. The *y*-axis represents the time interval for pH decline of the assay medium from 8.3 to 6.3.

In the plateaus, the equilibrium $10^3 \cdot \ln\alpha_{BaCO_3-H_2O}$ value averages $30.6 \pm 0.2$ for TS1 control experiments ($n = 8$) and $30.4 \pm 0.2$ for TS2 control experiments ($n = 10$). Our equilibrium $10^3 \cdot \ln\alpha_{BaCO_3-H_2O}$ value for TS2 control experiments at pH ~8.9 is consistent with Beck et al. (2005), who found a value of 30.46 from a $BaCO_3$ sample quantitatively precipitated from a $NaHCO_3$ solution at pH 8.93 fully equilibrated at 25 °C. Based on Zeebe (2007), the equilibrium $10^3 \cdot \ln\alpha_{BaCO_3-H_2O}$ value is expected to be 31.0 at pH 8.3 and 30.8 at pH 8.9. These are in reasonable agreement with the experimental data. General agreement between empirical data and theoretical calculations observed here demonstrate that our experimental approach is capable of reflecting the kinetics of the oxygen isotope exchange and equilibrium $^{18}O$ fractionations in the $CO_2$–$H_2O$ system.

*4.2.3. CA experiments*

Fig. 5 compares the results from control experiments and CA experiments at pH ~8.3 and ~8.9. At both pH levels, CA addition to the parent $NaHCO_3$ solutions accelerated the $^{18}O$ equilibration process. Furthermore, the time necessary for $^{18}O$ equilibration decreases with CA concentration. For example, the $^{18}O$ equilibration time is nearly halved when CA is present in the $NaHCO_3$ solution at concentration of $3.7 \times 10^{-9}$ M. These results exemplify the effect of CA on the $^{18}O$ exchange in the $CO_2$–$H_2O$ system via catalysis of $CO_2$ hydration. And importantly, the catalytic ability of CA was preserved even at pH ~8.9 which is comparable to the typical pH values within the calcification sites.

Fig. 6 compares the average equilibrium $\alpha_{BaCO_3-H_2O}$ values that are calculated from the data from the well-defined plateaus revealed in Fig. 5 and expected equilibrium $\alpha_{BaCO_3-H_2O}$ values at pH 8.3 and 8.9 from Zeebe (2007). The figure shows that the average equilibrium $\alpha_{BaCO_3-H_2O}$ values are indistinguishable at both pH levels, regardless of the presence or concentrations of CA in the parent $NaHCO_3$ solutions. Moreover, the equilibrium $\alpha_{BaCO_3-H_2O}$ values from control and CA experiments are in reasonable agreement with the expected values.

## 5. DISCUSSION

### 5.1. Kinetic rate constant for $CO_2$ hydroxylation reaction ($k_{+4}$)

The rate of $^{18}O$ equilibration is controlled by kinetic rate constants for $CO_2$ hydration ($k_{+2}$) and hydroxylation reaction ($k_{+4}$) and the pH-dependent DIC speciation (Eqs. (1)–(5)). For their study, Usdowski et al. (1991) used the temperature dependency of $k_{+4}$ by Pinsent et al. (1956). Recently Wang et al. (2010) published a new set of $k_{+4}$ data for a range of temperatures from 6.6 to 42.8 °C using the spectrophotometric stopped-flow method. The temperature dependency based on their new experimental results is given in Eq. (8). But their $k_{+4}$ measurements are greater than previously established values (including the ones by Pinsent et al., 1956) by a factor of about 2. Wang et al. (2010) did not thoroughly investigate the potential cause(s) for the offset between their $k_{+4}$ measurements and previous values mainly from 1950s and 1960s (original references therein), yet they commented that "considering the difficulties in the determination of this fast rate constant and the lack of available instrumentation some 50 years ago when

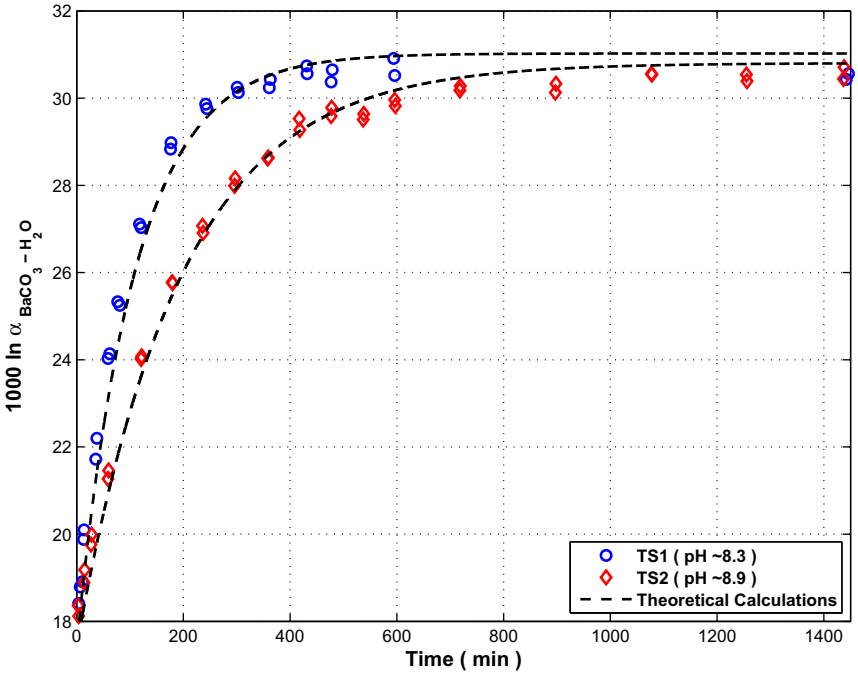


Fig. 4. Comparison of the results from control experiments without CA addition (TS1 series at pH 8.3 and TS2 series at pH 8.9) and theoretical time evolution of $\alpha_{S-H_2O}$ at respective pH levels (see Eq. (14)). Estimated time for 99% completion of $^{18}O$ equilibration ($t_{99\%}$) is about 480 and 900 min at pH 8.3 and 8.9, respectively.

most of the values were published, the analysis presented here is more likely the most reliable."

The results from our TS2 control experimental series can be used to indirectly evaluate the fidelity of the conflicting $k_{+4}$ values by Pinsent et al. (1956) and Wang et al. (2010). Since $CO_2$ hydroxylation is comparatively more important at higher pH, the results from our TS2 control experiments are better suited for the purpose. From the definition of the oxygen isotope fractionation factor α between $BaCO_3$ (and hence the sum of DIC species) and $H_2O$ (Eq. (12)), the rate expression for the $^{18}O$ exchange between DIC and $H_2O$ (Eq. (1)) can be rearranged to:

$$\ln\left(\frac{\alpha_{BaCO_3-H_2O}-\alpha^{EQ}_{BaCO_3-H_2O}}{\alpha^{0}_{BaCO_3-H_2O}-\alpha^{EQ}_{BaCO_3-H_2O}}\right)=-\left(\frac{1}{\tau}\right).t \quad (13)$$

which can be subsequently solved for $\alpha_{S-H_2O}$:

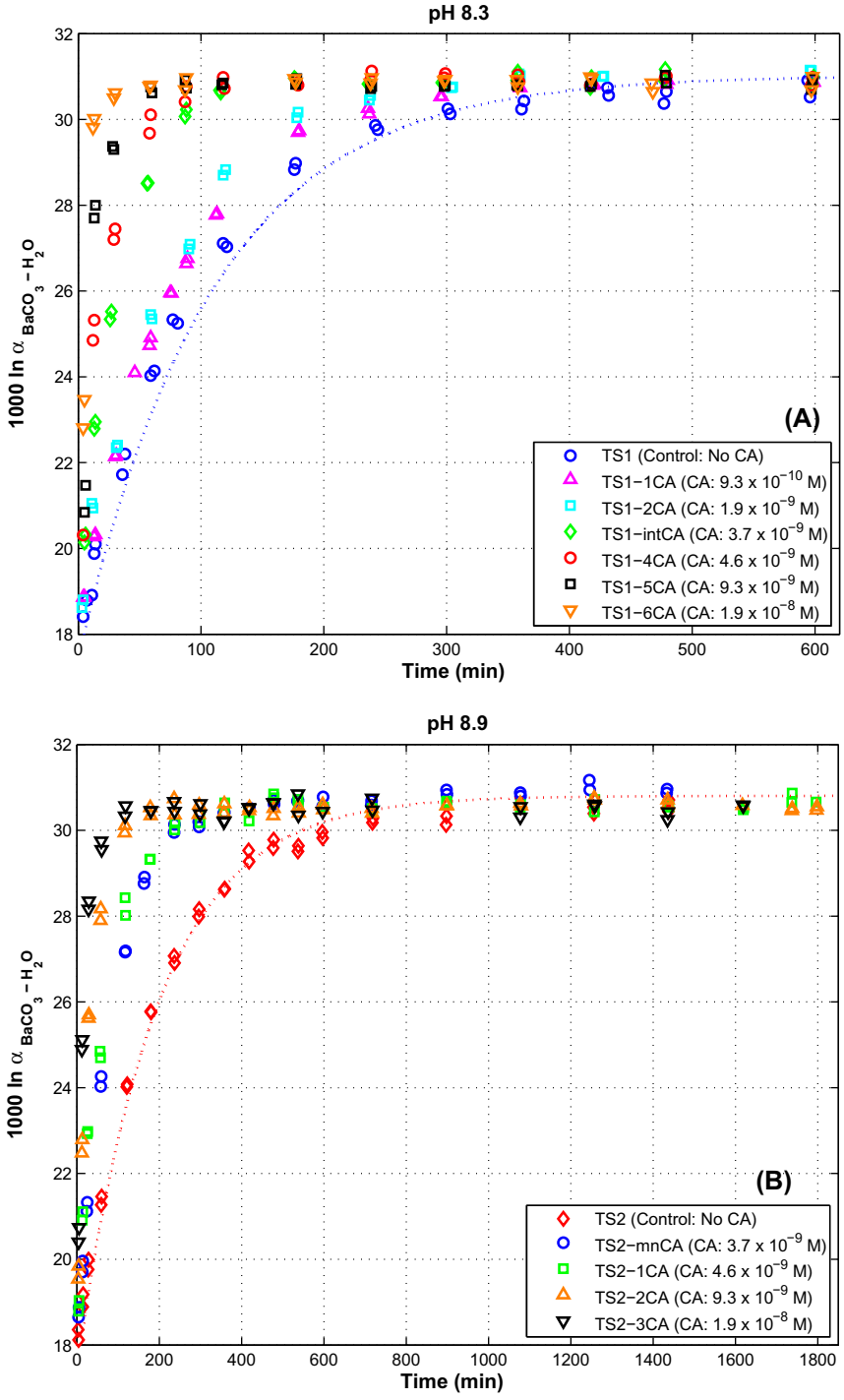


Fig. 5. Summary of the results from control experiments and CA experiments at pH 8.3 and 8.9. At both pH levels, the time required for $^{18}O$ equilibration in the $CO_2$–$H_2O$ system decreased with CA concentration.

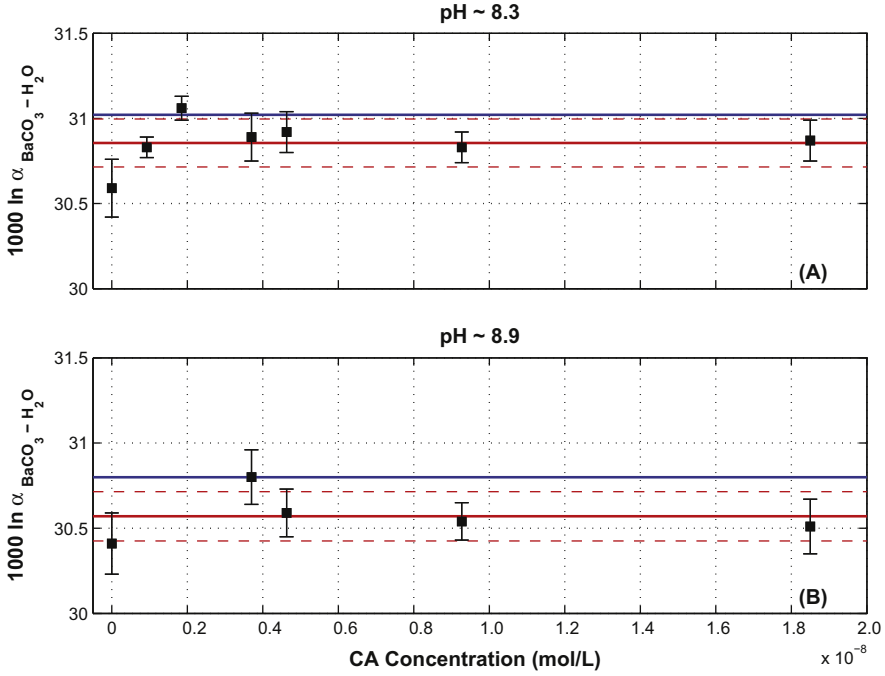


Fig. 6. The average equilibrium $\alpha_{S-H_2O}$ values as a function of CA concentration (Black). These values were calculated from the $\delta^{18}O$ values of the $BaCO_3$ samples precipitated after the $CO_2$–$H_2O$ system reached $^{18}O$ equilibrium, which is represented by the well defined plateaus in Fig. 5. The error bars represent $1\sigma$ standard deviations. (Red) The average and the $1\sigma$ standard deviations of the averaged equilibrium $\alpha_{S-H_2O}$ values shown by the black symbols in the plot. (Blue) Expected equilibrium $\alpha_{S-H_2O}$ values at pH 8.3 and 8.9 calculated from Zeebe (2007). (For interpretation of the references to colour in this figure legend, the reader is referred to the web version of this article.)

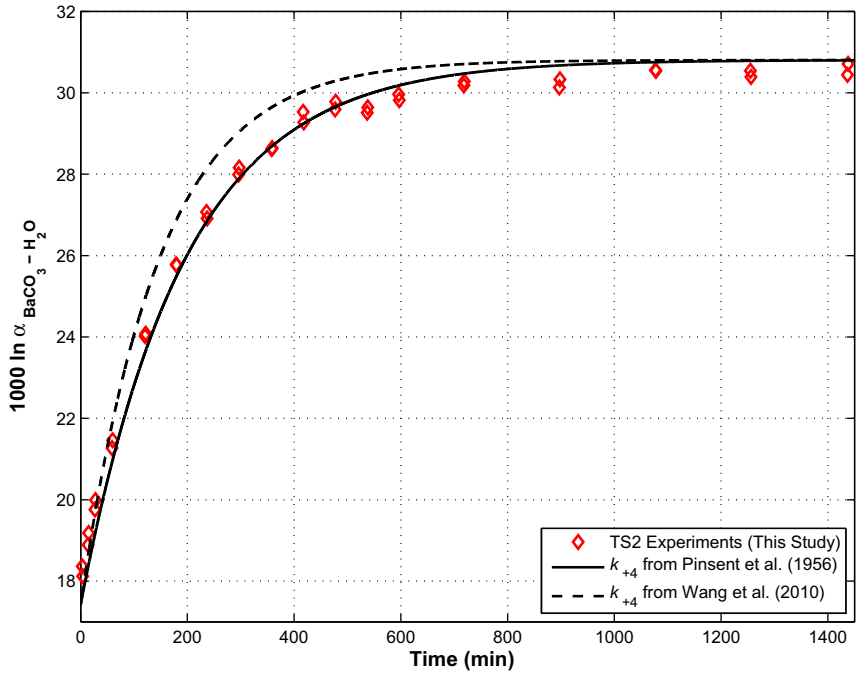


Fig. 7. Comparison of the results from TS2 control experiments performed at pH 8.9 (red symbols) and theoretical time evolution of $\alpha_{S-H_2O}$ at pH 8.9 modeled by Eq. (14) using the kinetic rate constant for $CO_2$ hydroxylation $k_{+4}$ by Pinsent et al. (1956) (solid curve) and by Wang et al. (2010) (dashed curve). (For interpretation of the references to colour in this figure legend, the reader is referred to the web version of this article.)

$$\alpha_{BaCO_3-H_2O} = \alpha^{EQ}_{BaCO_3-H_2O} + (\alpha^{0}_{BaCO_3-H_2O} - \alpha^{EQ}_{BaCO_3-H_2O}) \cdot \exp(-\frac{t}{\tau}) \quad (14)$$

This equation enables modeling of the time evolution of $\alpha_{BaCO_3-H_2O}$ from the initial condition $\alpha^{0}_{BaCO_3-H_2O}$ to the equilibrium condition $\alpha^{EQ}_{BaCO_3-H_2O}$. The $\alpha^{0}_{BaCO_3-H_2O}$ value can be determined from the $\delta^{18}O$ of the $NaHCO_3$ used for the experiments ($\delta^{18}O_{VSMOW} = 14.5‰$) and the average $\delta^{18}O$ value of $H_2O$ for the TS2 experiments ($\delta^{18}O_{VSMOW} = -3.0‰$). The $\alpha^{EQ}_{BaCO_3-H_2O}$ values at pH 8.89 (average pH for individual experiments in TS2 series) can be calculated by using the formulation by Zeebe (2007).

Fig. 7 compares the data from the TS2 control experiments and the simulated time evolution of $^{18}O$ equilibration based on the $k_{+4}$ value at 25 °C from Pinsent et al. (1956) and from Wang et al. (2010). The greater $k_{+4}$ values given by Wang et al. (2010) predict more rapid oxygen isotope exchange via $CO_2$ hydroxylation and therefore much faster overall $^{18}O$ equilibration in the $CO_2$–$H_2O$ system in comparison to the estimate based on the $k_{+4}$ from Pinsent et al. (1956). This trend should be even more pronounced at higher pH levels. However, our TS2 data closely trace the time evolution modeled with the $k_{+4}$ by Pinsent et al. (1956). As mentioned above, Wang et al. (2010) compared their $k_{+4}$ data with previously published results from six experimental studies including Pinsent et al. (1956). The $k_{+4}$ values from these six studies are in good agreement (see Fig. 6 in the supplementary online material by Wang et al., 2010). In fact, the $k_{+4}$ measurements below 16 °C by Wang et al. (2010) are also consistent with these studies. But above 25 °C, their measurements are anomalously higher than the data from previous studies. The evidence from our TS2 data and the consistent $k_{+4}$ measurements in previous experimental studies lead us to conclude that the values given by Wang et al. (2010) are overestimated. This suggests that the work by Pinsent et al. (1956) is more reliable.

### 5.2. Effect of CA on the equilibrium $^{18}O$ fractionation in the $CO_2$–$H_2O$ system

By definition, enzymes accelerate chemical reactions by lowering the activation energy. Hence the catalytic activity of CA is not expected to alter the equilibrium $^{18}O$ fractionations between DIC species and $H_2O$. But this might not be the case if CA itself or its derivatives such as amino acids or some type of degraded products form complexes with DIC species. From Fig. 6, however, the average equilibrium $\alpha_{BaCO_3-H_2O}$ values are generally consistent throughout the range of CA concentrations tested in this study. These experimentally-derived equilibrium $\alpha_{BaCO_3-H_2O}$ values are also very similar to the expected values (Zeebe, 2007). These lines of evidence suggest that the presence of CA does not affect the equilibrium $^{18}O$ fractionation in the range of CA concentration investigated in this study.

### 5.3. Effect of CA on the kinetics of $^{18}O$ equilibration

In the discussion above, we demonstrated that the uncatalyzed $^{18}O$ equilibration in the $CO_2$–$H_2O$ system can be explained by the mathematical model given in Usdowski et al. (1991) (Eqs. (3)–(5)). But as shown in Fig. 5, CA accelerates the oxygen isotope exchange by catalyzing $CO_2$ hydration and the exchange rate increases with CA concentration. In order to apply the model to our results from CA experiments, a new kinetic parameter needs to be implemented to account for the catalyzed $CO_2$ hydration. Boyer (1959) derived a rate expression for the catalyzed isotope exchange as a function of enzyme concentration, which was applied in Silverman (1973) to describe the influence of CA on the $^{18}O$ exchange between $HCO_3^-$ and $CO_2$. But some of the parameters such as equilibrium dissociation constant for the enzyme–substrate complex included in this expression are specific to the types of CA and these data are rarely reported in the literature. For our experimental conditions, a similar yet simpler parameterization can be employed.

A generalized expression for chemical reactions catalyzed by active enzymes can be written as:

$$E + S \underset{k-}{\overset{k+}{\rightleftharpoons}} EX \overset{k_{Cat}}{\rightarrow} E + P \quad (15)$$

where E, S and P denote the enzyme, substrate and product associated with the reaction, respectively. The notation EX represents the enzyme–substrate complex. The forward and reverse rate constant for the enzyme–substrate binding are denoted as $k_+$ and $k_-$, respectively. Finally $k_{Cat}$ is the catalytic rate constant, often referred to as the turnover number. In case of the $CO_2$ hydration catalyzed by CA, the substrate and product for the reaction would be $CO_{2(aq)}$ and $HCO_3^-$, respectively. Following the Michaelis–Menten kinetic model, the rate of increase in the product $HCO_3^-$ due to the catalyzed $CO_2$ hydration can be written as:

$$\frac{d[HCO_3^-]}{dt} = k_{Cat} \cdot [CA] \cdot \frac{[CO_2]}{K_M + [CO_2]} \quad (16)$$

where $K_M$ is the Michaelis–Menten constant ($K_M = (k_- + k_{Cat})/k_+$). Note that in our approach the contribution of the dehydration reaction ($HCO_3^- \rightarrow CO_2$) is automatically taken into account. The system is in chemical equilibrium, although not in isotopic equilibrium (see Appendix A). Between pH 8 and 9, $k_{Cat}$ appears to be independent of pH (Steiner et al., 1975). At 25 °C, $K_M$ of CA purified from bovine erythrocytes is also constant at $\sim 12 \times 10^{-3}$ M between pH 7 and 10 (DeVoe and Kistiakowsky, 1960; Kernohan, 1965; Pocker and Bjorkquist, 1977; Dodgson et al., 1990). Based on the algorithm of Zeebe and Wolf-Gladrow (2001), $[CO_{2(aq)}]$ in the parent $NaHCO_3$ solutions is $9.0 \times 10^{-5}$ M at pH 8.3 and $1.9 \times 10^{-5}$ M at pH 8.9. Hence $K_M \gg [CO_2]$ in our experimental condition and Eq. (16) can be approximated by:

$$\frac{d[HCO_3^-]}{dt} = \frac{k_{Cat}}{K_M} \cdot [CA] \cdot [CO_2] \quad (17)$$

Furthermore, the rate of increase in $HCO_3^-$ due to the uncatalyzed $CO_2$ hydration is:

$$\frac{d[HCO_3^-]}{dt} = k_{+2} \cdot [CO_2] \quad (18)$$

Combining the contribution from the catalyzed and uncatalyzed $CO_2$ hydration, the total rate of increase in $HCO_3^-$ is:

$$\frac{d[HCO_3^-]}{dt} = \left(k_{+2} + \frac{k_{Cat}}{K_M}\cdot[CA]\right)\cdot[CO_2] \quad (19)$$

Thus, in order to account for the catalyzed and uncatalyzed $CO_2$ hydration, the time constant $\tau^{-1}$ (Eq. (5)) can be modified to:

$$\tau^{-1} = (0.5)\cdot\{k_{+2}^* + k_{+4}[OH^-]\} \cdot\left\{1 + \frac{[CO_2]}{S} - \left[1 + \left(\frac{2}{3}\cdot\frac{[CO_2]}{S}\right) + \left(\frac{[CO_2]}{S}\right)^2\right]^{1/2}\right\} \quad (20)$$

where $k_{+2}^*$ is the overall $CO_2$ hydration constant, which accounts for both uncatalyzed and catalyzed $CO_2$ hydration:

$$k_{+2}^* = k_{+2} + \frac{k_{Cat}}{K_M}\cdot[CA] \quad (21)$$

In Fig. 8 our experimental results are rearranged according to the left-hand side of Eq. (13). Note that the data presented here are limited to the early phase of $^{18}O$ equilibration (i.e., data from the regions where $\alpha_{BaCO_3-H_2O}$ values are rapidly changing with time in Fig. 7). This is because the $\ln\{(\alpha_{BaCO_3-H_2O} - \alpha^{EQ}_{BaCO_3-H_2O})/(\alpha^0_{BaCO_3-H_2O} - \alpha^{EQ}_{BaCO_3-H_2O})\}$ values calculated from the data in the plateaus are obscured by experimental uncertainties. Then the results can be nicely fit by linear regressions (Table 3). The $r^2$ values for the regressions were better than 0.95 except for the TS1-6CA experimental series ($r^2 = 0.83$). This is due to scarcity of the data points since the $^{18}O$ equilibration was very rapid at this experimental condition relative to our experimental resolution. The slopes obtained from the linear regressions are equivalent to the numerical values of the time constant $\tau^{-1}$, from which $k_{+2}^*$ can be calculated (see Eq. (20)).

Fig. 9 displays the dependency of $k_{+2}^*$ on the CA concentration in the parent $NaHCO_3$ solution. The relationship between $k_{+2}^*$ and CA concentration is best described by a linearity ($r^2 = 0.99$), as expected from Eq. (21). It should be noted that the intercept and the slope from the linear regression reflect $k_{+2}$ and $k_{Cat}/K_M$, respectively (Eq. (21)). The value of the intercept is 2.3 ($\pm$0.1) $\times 10^{-2}$ $s^{-1}$, which is in agreement with the uncatalyzed $k_{+2}$ of $2.6 \times 10^{-2}$ $s^{-1}$ by Pinsent et al. (1956) at 25 °C. Due to considerable variations in the $k_{Cat}$ values of bovine CA reported in the literature (e.g., Kernohan, 1965; Donaldson and Quinn, 1974; Pocker and Bjorkquist, 1977; Dodgson et al., 1990), the $k_{Cat}/K_M$ value for bovine erythrocyte CA at 25 °C may vary between $2.3 \times 10^7$ and $8.3 \times 10^7$ $M^{-1}$ $s^{-1}$ based on the $K_M$ value of $12 \times 10^{-3}$ M. The $k_{Cat}/K_M$ value obtained from our experimental results is 2.7 ($\pm$0.1) $\times 10^7$ $M^{-1}$ $s^{-1}$, which fits into the expected range. This suggests that our experimental results are consistent with the theoretical constraints based on the fundamental kinetic principles.

Our experiments were performed at 25 °C. However, the equilibrium constants and uncatalyzed kinetic rate constants applied in our model are well established for temperature range from 0 to 40 °C or so (Table 1). Also the $k_{Cat}/K_M$ of bovine CA appears to be unaffected by temperature from 5 to 30 °C (Ghannam et al., 1986). Therefore our experimental results can be extrapolated to the typical range of oceanic temperatures in which majority of biogenic calcification takes place. In addition, the parameterization of the catalyzed $CO_2$ hydration using the $k_{Cat}/K_M$ in our

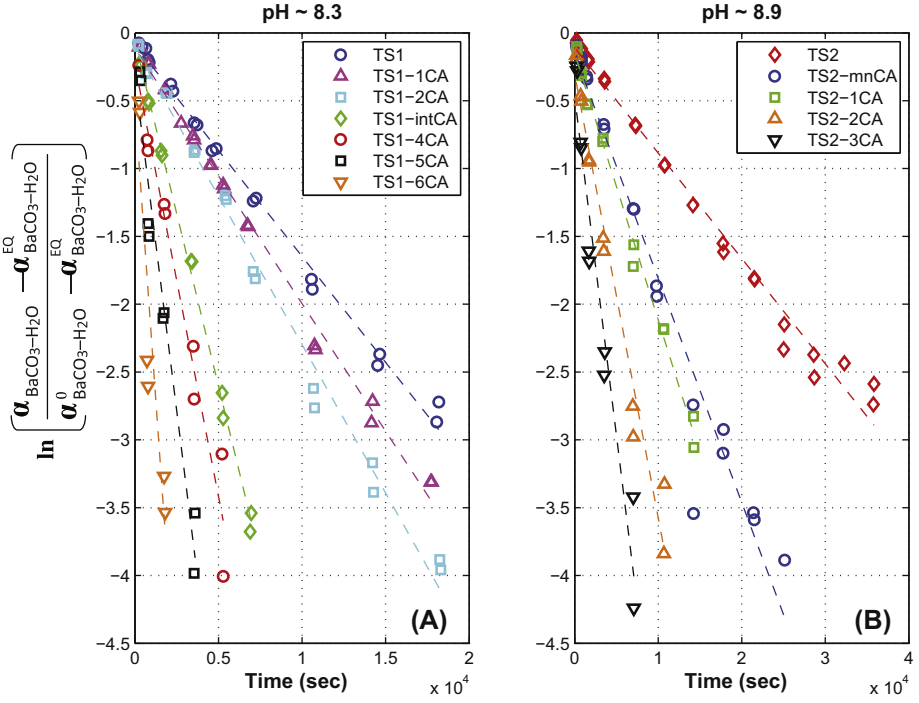


Fig. 8. Linear regressions of the experimental results following Eq. (13). The slopes from the regressions (see Table 3) are equivalent to the numerical values of the time constant $-\tau^{-1}$ (Eq. (20)).

Table 3
The results of linear regressions of the experimental results against time following Eq. (13) (see Fig. 8). The slopes obtained from the regressions are equivalent to the numerical values of the time constant $-\tau^{-1}$ (Eq. (20)).

| Experiment series | Slope ($s^{-1}$) | Slope $\sigma^{\dagger}$ | Intercept | Intercept $\sigma^{\dagger}$ | $r^2$ |
|---|---|---|---|---|---|
| TS1 (Control) | $-1.56 \times 10^{-4}$ | $2.96 \times 10^{-6}$ | −0.09 | 0.03 | 0.99 ($n = 19$) |
| TS1-1CA | $-1.88 \times 10^{-4}$ | $3.38 \times 10^{-6}$ | −0.11 | 0.03 | 0.99 ($n = 21$) |
| TS1-2CA | $-2.19 \times 10^{-4}$ | $5.28 \times 10^{-6}$ | −0.11 | 0.05 | 0.99 ($n = 18$) |
| TS1-intCA | $-5.08 \times 10^{-4}$ | $8.63 \times 10^{-6}$ | −0.06 | 0.03 | 1.00 ($n = 12$) |
| TS1-4CA | $-6.37 \times 10^{-4}$ | $4.90 \times 10^{-5}$ | −0.23 | 0.15 | 0.96 ($n = 9$) |
| TS1-5CA | $-9.85 \times 10^{-4}$ | $8.97 \times 10^{-5}$ | −0.32 | 0.18 | 0.95 ($n = 8$) |
| TS1-6CA | $-1.75 \times 10^{-3}$ | $3.90 \times 10^{-4}$ | −0.53 | 0.44 | 0.83 ($n = 6$) |
| TS2 (Control) | $-7.77 \times 10^{-5}$ | $2.06 \times 10^{-6}$ | −0.11 | 0.04 | 0.98 ($n = 24$) |
| TS2-mnCA | $-1.65 \times 10^{-4}$ | $8.87 \times 10^{-6}$ | −0.16 | 0.11 | 0.96 ($n = 19$) |
| TS2-1CA | $-1.97 \times 10^{-4}$ | $4.84 \times 10^{-6}$ | −0.15 | 0.04 | 0.99 ($n = 14$) |
| TS2-2CA | $-3.27 \times 10^{-4}$ | $1.80 \times 10^{-6}$ | −0.30 | 0.10 | 0.97 ($n = 12$) |
| TS2-3CA | $-5.00 \times 10^{-4}$ | $4.29 \times 10^{-5}$ | −0.47 | 0.16 | 0.94 ($n = 10$) |

$^{\dagger}$ Standard error of the slope and intercept calculated from Higbie (1991).

model is highly practical. Since the $k_{Cat}/K_M$ is a primary measure of the catalytic efficiency of an enzyme, this parameter is routinely determined in enzymatic studies. Hence the kinetics of the $^{18}O$ exchange in the $CO_2$–$H_2O$ system catalyzed by different classes of CA other than bovine CA can be readily modeled with the $k_{Cat}/K_M$ data.

### 5.4. Implications for $\delta^{18}O$ vital effects in marine biogenic carbonates

Two different models have been proposed as an explanation for $^{18}O$ depletion in biogenic $CaCO_3$. McConnaughey (1989a, 1989b, 2003) argued that $^{18}O$-depletion as a result of the kinetic effects associated with $CO_2$ hydration and hydroxylation could be recorded in $CaCO_3$ if the precipitation rate is faster than $^{18}O$ equilibration in the $CO_2$–$H_2O$ system. On the other hand Zeebe (1999, 2007) argued that $\delta^{18}O$ vital effects are largely due to the role of fluid pH in defining the DIC speciation and consequently the overall $\delta^{18}O$ signature of the sum of DIC species. Corals are capable of maintaining elevated pH levels in the extracellular calcifying fluid from which calcification proceeds (Al-Horani et al., 2003; Rollion-Bard et al., 2003, 2011). Foraminifera can also maintain strong pH gradients between intracellular fluid and ambient seawater (Rink et al., 1998; Köhler-Rink and Kühl, 2005; de Nooijer et al., 2009; Bentov et al., 2009; Rollion-Bard and Erez, 2010). Hence the pH control on the overall $\delta^{18}O$ of the sum of DIC species in such alkaline fluid may be important for $^{18}O$ depletion in biogenic $CaCO_3$ with respect to anticipated $\delta^{18}O$ values that are in thermodynamic equilibrium with ambient seawater (Adkins et al., 2003; Rollion-Bard et al., 2003).

A crucial aspect for both the kinetic-based and pH-based model is the balance between the rate of DIC utilization for calcification and the rate of $^{18}O$ equilibration in the $CO_2$–$H_2O$ system. If the equilibration process is sufficiently rapid, the $HCO_3^-$ and $CO_3^{2-}$ ions that are potentially depleted in $^{18}O$ due to the kinetic effects can re-establish local $^{18}O$ equilibrium in the calcification sites and thus no kinetic effects would occur. The counter-argument for the pH model points to the question whether $^{18}O$ equilibrium in the $CO_2$–$H_2O$ system can be established quickly enough at elevated pH levels in the calcification sites (recall that equilibration takes considerably longer at higher pH as shown in Fig. 1).

In this study, we experimentally demonstrated that the $^{18}O$ equilibration process is accelerated by the presence of small amounts of CA due to its ability to catalyze the $CO_2$ hydration reaction (Fig. 5). In addition, the catalytic ability of the enzyme can be fully expressed even at elevated pH at 8.9 that is typical for the calcification sites. These findings support the notion that the $^{18}O$ equilibrium in the calcification sites is feasible. However, this idea requires the presence of extracellular CA in the actual calcification sites. Another crucial requirement is that the CA in these organisms needs to be as active and efficient as the purified bovine CA used in our experiments.

Several studies provide direct evidence for the presence of extracelluar CA in the coral calcification sites (Furla et al., 2000; Tambutté et al., 2006; Moya et al., 2008). Particularly Moya et al. (2008) isolated extracellular CA named STPCA in the calcification sites of a symbiotic branching scleractinian coral *Stylophora pistillata* and analyzed the catalytic efficiency of the enzyme. Based on the measurement at 20 °C and pH 7.5, the $k_{Cat}/K_M$ value for STPCA was found to be $4.6 \times 10^7\ M^{-1}\ s^{-1}$. Despite intracellular presence in the oral endoderm and the aboral tissues, notably Bertucci et al. (2011) isolated another type of CA, STPCA-2, in the same coral species *S. pistillata*. It is worthwhile to emphasize that the catalytic efficiency of the STPCA-2 ($k_{Cat}/K_M = 8.3 \times 10^7\ M^{-1}\ s^{-1}$) is comparable to that of a human cytoplasmic CA (hCA-II type, $k_{Cat}/K_M = 1.5 \times 10^8\ M^{-1}\ s^{-1}$), which is classified as one of the most efficient and active form of CA (Bertucci et al., 2011). By applying the STPCA and STPCA-2 $k_{Cat}/K_M$ data, it is possible to calculate the time required for $t_{99\%}$ (Eq. (6)) as a function of concentration of these enzymes using Eqs. (6), (20), and (21). Under uncatalyzed condition, $t_{99\%}$ is roughly 900 min at pH 8.9 (Table 4). But with the presence of only as little as $9.3 \times 10^{-10}$ M of STPCA and STPCA-2, the $t_{99\%}$ will be reduced to roughly 620 and

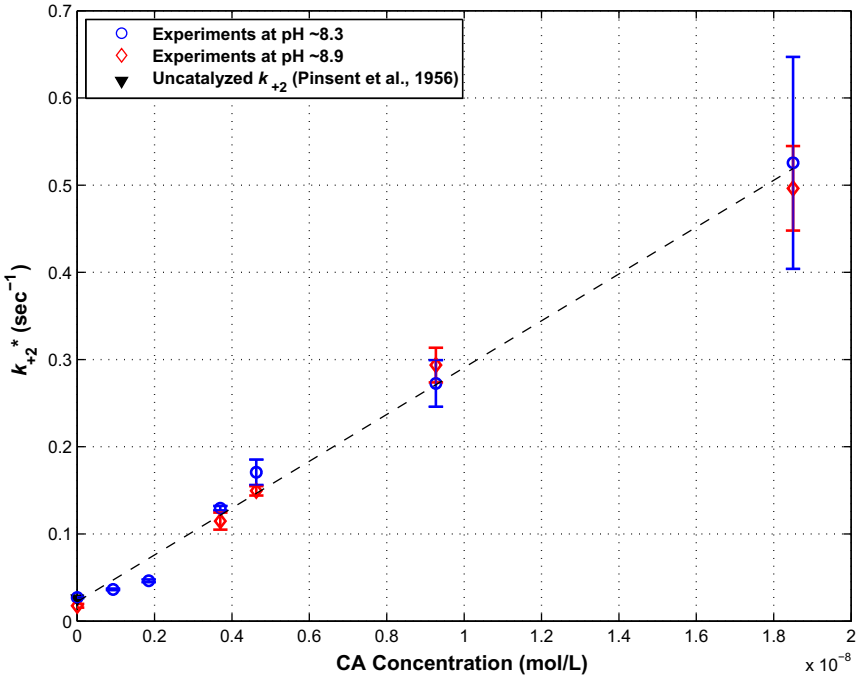


Fig. 9. The effect of CA concentration on the overall $CO_2$ hydration constant $k_{+2}^*$ (Eqs. (18) and (19)), which accounts for both the uncatalyzed and catalyzed $CO_2$ hydration. The error bars indicate the propagated errors in the $-\tau^{-1}$ values based on the linear regressions of the experimental results (Table 3). The dashed line represents the linear regression for all of the data points in the figure. The intercept of the regression line is equivalent to the kinetic rate constant for the uncatalyzed $CO_2$ hydration $k_{+2}$. The slope reflects the $k_{Cat}/K_M$ of the CA used in this experiment. The $k_{+2}$ from our experimental results are in good agreement with Pinsent et al. (1956).

500 min, respectively. These are approximately 30% and 45% reduction from the uncatalyzed $^{18}O$ equilibration time. If these enzymes are present at $1.9 \times 10^{-8}$ M, which represents the maximum CA concentration tested in this study, the 99% equilibration time will be shortened to about 90 min for STPCA and 50 min for STPCA-2.

Are these estimates of the influence of STPCA and STPCA-2 on $^{18}O$ equilibration relevant to the realistic timescales of biogenic calcification? McConnaughey (2003) suggested that the residence time of DIC in the coral calcification site can be estimated by:

$$\text{DIC Residence Time} = [\text{DIC}] \cdot h \cdot R^{-1} \quad (22)$$

where $h$ is the thickness of the calcifying space and $R$ is the calcification rate. By employing $[\text{DIC}] = 2 \times 10^3$ mol/m$^3$, $h = 10^{-6}$ m and $R = 10^{-7}$ mol/m$^{-2}$/s after McConnaughey (2003), the DIC residence time in the coral calcification sites appears to be on the order of 5.5 h. This should be sufficient for the $CO_2$–$H_2O$ system in calcification site to reach $^{18}O$ equilibrium, if the system is catalyzed by only $\sim 3 \times 10^{-9}$ M of CA that is as effective as STPCA and STPCA-2 (see Table 4).

One caveat in the discussion above is the potential influence of possible activators/inhibitors on the kinetic properties ($k_{Cat}/K_M$) of extracellular CA *in vivo*. For example, Bertucci et al. (2010) demonstrated that certain amino acids and amines can act as activators and increases $k_{Cat}$ of STPCA. On the contrary, STPCA activity can be inhibited by certain inorganic anions (Bertucci et al., 2009). Our calculations of $t_{99\%}$ using the $k_{Cat}/K_M$ values of STPCA and STPCA-2 (Table 4) do not account for these factors, which could be important in the actual calcification sites. Another critical unknown is the actual concentrations or the total extracellular CA activities in the calcification sites. We note, however, that the study by Tambutté et al. (2006) marks an important step forward in this respect. They performed enzyme assay and measured the extracellular CA activity in the soluble proteins extracted from the skeletal organic matrix of a non-symbiotic coral *Tubastrea aurea*. In case of foraminifera, the presence of CA has not been unequivocally confirmed. ter Kuile et al. (1989) observed reduced calcification and photosynthetic rate in *Amphistegina lobifera* and *Amphisorus hemprichii* cultured with a CA-inhibitor (ethoxyzolamide). Although this finding supports the presence of CA in some foraminiferal species, the localities, catalytic properties and concentrations of CA still need to be clarified.

But at this point, the presence and robust activity of extracellular CA and its direct involvement in the calcification are inarguable at least in some corals (e.g., Furla et al., 2000; Moya et al., 2008; Tambutté et al., 2011). Based on these lines of evidence, establishment of $^{18}O$ equilibrium in the calcification sites is possible depending on the actual concentrations of CA such as STPCA and STPCA-2. In that case $^{18}O$-depletion in DIC species (namely in $HCO_3^-$ and $CO_3^{2-}$) resulting from the kinetic effect associated with $CO_2$ hydration and hydroxylation can be eliminated, which is crucial for comprehensive understanding of $\delta^{18}O$ vital effects. Evaluation of this hypothesis requires inputs from future research, which should focus on identification, characterization and quantification of extracellular CA in marine calcifiers.

Table 4
Comparison of the effect of concentration and the type of CA on the time required for 99% completion of $^{18}O$ equilibration ($t_{99\%}$) in the $CO_2$–$H_2O$ system at pH 8.9 and at 25 °C. The estimates are based on the mathematical model developed in this study (see Eqs. (6), (20), and (21)).

| CA conc. (M: mol/L) | $t_{99\%}$ (min.) | | |
|---|---|---|---|
| | Bovine CA* | STPCA† | STPCA-2‡ |
| 0 | 904.7 | 904.7 | 904.7 |
| $9.3 \times 10^{-10}$ | 715.1 | 621.7 | 496.7 |
| $1.9 \times 10^{-9}$ | 591.6 | 474.1 | 342.8 |
| $3.7 \times 10^{-9}$ | 439.5 | 321.2 | 211.5 |
| $4.6 \times 10^{-9}$ | 389.2 | 276.4 | 177.3 |
| $9.3 \times 10^{-9}$ | 247.7 | 163.0 | 98.2 |
| $1.9 \times 10^{-8}$ | 143.8 | 89.7 | 52.0 |

* For bovine erythrocyte CA, the $k_{Cat}/K_M$ value of $2.7 \times 10^7\ M^{-1}\ s^{-1}$ from our experimental results was used for the estimates (Fig. 9).
†,‡ The estimates are based on the $k_{Cat}/K_M$ value of $4.6 \times 10^7\ M^{-1}\ s^{-1}$ for STPCA (Moya et al., 2008) and $8.3 \times 10^7\ M^{-1}\ s^{-1}$ for STPCA-2 (Bertucci et al., 2011). These $k_{Cat}/K_M$ values were determined at pH 7.5 and at 20 °C (see the original references for details). No further corrections on the $k_{Cat}/K_M$ values were made for the $t_{99\%}$ estimates presented here.

## 6. CONCLUSIONS

We have performed quantitative $BaCO_3$ precipitation experiments to quantify the effect of CA on the kinetics and equilibrium of the $^{18}O$ exchange in the $CO_2$–$H_2O$ system. The results from our control experiments indicate that the uncatalyzed evolution of $^{18}O$ equilibrium can be modeled by the mathematical expression given in Usdowski et al. (1991), which is derived in Appendix A. Furthermore, we find that the recently published kinetic rate constant for $CO_2$ hydroxylation by Wang et al. (2010) is inconsistent with our results as well as previously published rate constants. We argue that the measurements by Wang et al. (2010) are most likely overestimates. When CA is present in the $CO_2$–$H_2O$ system, the time required for $^{18}O$ equilibrium is greatly reduced due to the catalysis of $CO_2$ hydration and its reverse reaction. On the other hand, CA does not alter the equilibrium oxygen isotope fractionation in the $CO_2$–$H_2O$ system. Under our experimental conditions, the catalysis of the $CO_2$ hydration by CA can be parameterized by the $k_{Cat}/K_M$ and the total enzyme concentration. Given the evidence for the presence of highly active CA such as STPCA and STPCA-2 (Moya et al., 2008; Bertucci et al., 2011), it is possible that $^{18}O$ equilibration of the $CO_2$–$H_2O$ system can outpace the DIC utilization in the calcification sites. We therefore argue that the catalytic role of CA may be of critical importance in developing a realistic model of $\delta^{18}O$ vital effects in biogenic $CaCO_3$.

### ACKNOWLEDGMENTS

We are grateful to Howie Spero, David Winter, Spider Vetter (UC Davis) and Dyke Andreasen (UC Santa Cruz) for stable isotope analyses. The Univ. of Hawaii at Hilo XRD Facility is also thanked for analytical service. J. Uchikawa thanks his dissertation committee (B.N. Popp, Y.-H. Li, G.E. Ravizza and J.E. Schoonmaker) for constructive criticism. This paper benefited from the comments by the associate editor (Dr. Claire Rollion-Bard), Ted McConnaughey and two anonymous reviewers. This research was supported by the U.S. National Science Foundation (Grants OCE05-25647 and OCE09-27089). SOEST contribution #8728.

## APPENDIX A

Derivation of the rate law for the oxygen isotope exchange in the $CO_2^-$–$H_2O$ system via uncatalyzed $CO_2$ hydration and hydroxylation.

Usdowski et al. (1991) gave their rate expression without describing the derivation process. In this appendix we show that the expression can be derived by following the scheme presented in Mills and Urey (1940). In this classical paper, an expression for the rate of $^{18}O$ exchange involved in $CO_2$ hydration reaction was introduced.

For $CO_2$ hydration, simple chemical equilibrium can be written as:

$$CO_2 + H_2O \underset{k_{-2}}{\overset{k_{+2}}{\rightleftarrows}} H_2CO_3 \tag{A-1}$$

where $k_{+2}$ and $k_{-2}$ are the kinetic rate constant for the forward and reverse (dehydration) reaction. By applying a simple numeric notation 6 and 8 for the $^{16}O$ and $^{18}O$ isotopes in $CO_2$, $H_2O$ and $H_2CO_3$ (e.g., Gao and Marcus, 2001), the oxygen isotope equilibration for the same reaction can be written as:

$$(66) + (6) \underset{k_{-2}}{\overset{k_{+2}}{\rightleftarrows}} (666) \tag{A-1a}$$

$$(66) + (8) \underset{k_{-2}}{\overset{k_{+2}}{\rightleftarrows}} (668) \tag{A-1b}$$

$$(68) + (6) \underset{k_{-2}}{\overset{k_{+2}}{\rightleftarrows}} (668) \tag{A-1c}$$

$$(68) + (8) \underset{k_{-2}}{\overset{k_{+2}}{\rightleftarrows}} (688) \tag{A-1d}$$

$$(88) + (6) \underset{k_{-2}}{\overset{k_{+2}}{\rightleftarrows}} (688) \tag{A-1e}$$

$$(88) + (8) \underset{k_{-2}}{\overset{k_{+2}}{\rightleftarrows}} (888) \tag{A-1f}$$

where $(6) = H_2{}^{16}O$, $(68) = C^{16}O^{18}O$, $(668) = H_2C^{16}O^{16}O^{18}O$ and so on. Following Mills and Urey (1940), the rate of change in the $^{18}O$ content of $CO_2$ can be expressed as:

$$-\frac{d^{18}O(CO_2)}{dt} = k_{+2}[68][6] + k_{+2}[68][8] + 2k_{+2}[88] \times [6] + 2k_{+2}[88][8] - \frac{2}{3}k_{-2}[668] - \frac{4}{3}k_{-2}[688] - 2k_{-2}[888], \tag{A-2a}$$

which can be rearranged to:

$$-\frac{d^{18}O(CO_2)}{dt} = k_{+2}\{[6] + [8]\}\{[68] + 2[88]\} - 2k_{-2}\left\{\frac{1}{3}[668] + \frac{2}{3}[688] + [888]\right\} \tag{A-2b}$$

However, oxygen isotope exchange associated with $CO_2$ hydroxylation also needs to be taken into account for the $CO_2$–$H_2O$ system when pH > 7. By adopting a notation such as (6)′ and (888)′ to differentiate the $^{16}O$ and $^{18}O$ isotopes in $OH^-$ and $HCO_3^-$ ions from $H_2O$ and $H_2CO_3$, the chemical equilibrium and associated oxygen isotope equilibration for the $CO_2$ hydroxylation reaction can be similarly written as:

$$CO_2 + OH^- \underset{k_{-4}}{\overset{k_{+4}}{\rightleftarrows}} HCO_3^- \tag{A-3}$$

and:

$$(66) + (6)' \underset{k_{-4}}{\overset{k_{+4}}{\rightleftarrows}} (666)' \tag{A-3a}$$

$$(66) + (8)' \underset{k_{-4}}{\overset{k_{+4}}{\rightleftarrows}} (668)' \tag{A-3b}$$

$$(68) + (6)' \underset{k_{-4}}{\overset{k_{+4}}{\rightleftarrows}} (668)' \tag{A-3c}$$

$$(68) + (8)' \underset{k_{-4}}{\overset{k_{+4}}{\rightleftarrows}} (688)' \tag{A-3d}$$

$$(88) + (6)' \underset{k_{-4}}{\overset{k_{+4}}{\rightleftarrows}} (688)' \tag{A-3e}$$

$$(88) + (8)' \underset{k_{-4}}{\overset{k_{+4}}{\rightleftarrows}} (888)' \tag{A-3f}$$

Following the approach by Mills and Urey (1940), the rate of change in the $^{18}O$ content in $CO_2$ due to $CO_2$ hydroxylation is:

$$\begin{aligned} -\frac{d^{18}O(CO_2)}{dt} &= k_{+4}[68][6]' + k_{+4}[68][8]' + 2k_{+4}[88] \\ &\quad \times [6]' + 2k_{+4}[88][8]' - \frac{2}{3}k_{-4}[668]' \\ &\quad - \frac{4}{3}k_{-4}[688]' - 2k_{-4}[888]', \end{aligned} \tag{A-4a}$$

which can be rearranged to:

$$\begin{aligned} -\frac{d^{18}O(CO_2)}{dt} &= k_{+4}\{[6]' + [8]'\}\{[68] + 2[88]\} \\ &\quad - 2k_{-4}\left\{\frac{1}{3}[668]' + \frac{2}{3}[688]' + [888]'\right\} \end{aligned} \tag{A-4b}$$

From Eqs. A-2b and A-4b, the net rate of change in the $^{18}O$ content in $CO_2$ due to both $CO_2$ hydration and hydroxylation is:

$$\begin{aligned} -\frac{d^{18}O(CO_2)}{dt} &= k_{+2}\{[6] + [8]\}\{[68] + 2[88]\} \\ &\quad - 2k_{-2}\left\{\frac{1}{3}[668] + \frac{2}{3}[688] + [888]\right\} \\ &\quad + k_{+4}\{[6]' + [8]'\}\{[68] + 2[88]\} \\ &\quad - 2k_{-4}\left\{\frac{1}{3}[668]' + \frac{2}{3}[688]' + [888]'\right\} \end{aligned} \tag{A-5}$$

Similar rate equations can be set up for $H_2CO_3$ and $HCO_3^-$ using the expression for oxygen isotope equilibration via hydration and hydroxylation (Eqs. (A-1a–A-1f), (A-3a–A-3f)):

$$\begin{aligned} -\frac{d^{18}O(H_2CO_3)}{dt} &= k_{-2}[668] + 2k_{-2}[688] + 3k_{-2}[888] \\ &\quad - k_{+2}[66][8] - k_{+2}[68][6] \\ &\quad - 2k_{+2}[68][8] - 2k_{+2}[88][6] \\ &\quad - 3k_{+2}[88][8] \end{aligned} \tag{A-6}$$

$$\begin{aligned} -\frac{d^{18}O(HCO_3^-)}{dt} &= 3k_{-4}\left\{\frac{1}{3}[668]' + \frac{2}{3}[688] + [888]'\right\} \\ &\quad - k_{-4}[6]'\{[68] + 2[88]\} \\ &\quad - k_{-4}[8]'\{[66] + 2[68] + 3[88]\} \end{aligned} \tag{A-7}$$

Then we define $\alpha$, $\beta$, $\gamma$, $\varepsilon$ and $\theta$ as the atom fraction of the $^{18}O$ isotopes in $CO_2$, $H_2O$, $H_2CO_3$ and $HCO_3^-$ and $OH^-$:

$$\alpha = \frac{2[88] + [68]}{2[CO_2]} \tag{A-8}$$

$$\beta = \frac{[8]}{H_2O} \tag{A-9}$$

$$\gamma = \frac{[668] + 2[688] + 3[888]}{3[H_2CO_3]} \tag{A-10}$$

$$\varepsilon = \frac{[668]' + 2[688]' + 3[888]'}{3[HCO_3^-]} \tag{A-11}$$

$$\theta = \frac{[8]'}{OH^-} \tag{A-12}$$

Note that in (Eq. A-5) the term $\{[6] + [8]\}$ is essentially $\{[H_2{}^{16}O] + [H_2{}^{18}O]\}$, which is simply $[H_2O]$. Likewise, $\{[66] + 2[68]\}$ and $\{[6]' + [8]'\}$ are equal to $[CO_2]$ and $[OH^-]$, respectively. In addition, equilibrium constant ($K$) and kinetic rate constants ($k$) for a given chemical reaction are interrelated, such that for $CO_2$ hydration:

$$\begin{aligned} K_2 = \frac{[H_2CO_3]}{[CO_2][H_2O]} = \frac{k_{+2}}{k_{-2}} &\iff k_{-2}[H_2CO_3] \\ = k_{+2}[CO_2][H_2O] \end{aligned} \tag{A-13}$$

and for $CO_2$ hydroxylation:

$$\begin{aligned} K_4 = \frac{[HCO_3^-]}{[CO_2][OH^-]} = \frac{k_{+4}}{k_{-4}} &\iff k_{-4}[HCO_3^-] \\ = k_{+4}[CO_2][OH^-] \end{aligned} \tag{A-14}$$

Note that by using these relationships, the contribution of the dehydration reaction ($HCO_3^- \rightarrow CO_2$) is automatically taken into account in our approach (system is in chemical equilibrium, although not in isotopic equilibrium). After algebraic manipulations using the definitions for $\alpha$, $\gamma$ and $\varepsilon$ (Eqs. A-8–A-12) and the relationships described above, the rate equation for the change in $^{18}O$ content in $CO_2$, $H_2CO_3$ and $HCO_3^-$ (Eqs. A-5–A-7) can be rearranged to:

$$2[CO_2]\frac{d\alpha}{dt} = 2[CO_2]\{k_{+2}(\gamma - \alpha) + k_{+4}[OH^-](\varepsilon - \alpha)\} \tag{A-15}$$

$$3[H_2CO_3]\frac{d\gamma}{dt} = k_{+2}[CO_2](2\alpha + \beta - 3\gamma) \tag{A-16}$$

$$3[HCO_3^-]\frac{d\varepsilon}{dt} = k_{+4}[CO_2][OH^-](2\alpha + \theta - 3\varepsilon) \tag{A-17}$$

Note that [$H_2O$] terms in these equations are dropped because the [$H_2O$] contribution is already taken into account in the equilibrium ($K$) and kinetic constants ($k$) compiled by Usdowski et al. (1991), which are given in Table 1 of this paper. Also note that similar rate expressions for $\beta$ and $\theta$ can be established. However, the $^{18}O$ content of $H_2O$ is constant and $OH^-$ is in isotopic equilibrium with $H_2O$. Hence the rate expressions for these components do not require further considerations.

It is important to note that protonation and deprotonation reaction among $H_2CO_3$, $HCO_3^-$ and $CO_3^{2-}$ ions is a very rapid process ($\sim 10^{-7}$ s) relative to $CO_2$ hydration and hydroxylation reaction ($\sim$10 s) (Zeebe and Wolf-Gladrow, 2001). Consequently we can assume that the $^{18}O$ content in these particular DIC species at a given time over the course of $^{18}O$ equilibration of the $CO_2$–$H_2O$ system are inseparable, hence we need to consider total $^{18}O$ content in the sum of $H_2CO_3$, $HCO_3^-$ and $CO_3^{2-}$. Also note that an independent rate reaction for $^{18}O$ content in $CO_3^{2-}$ is not necessary. This is because $CO_3^{2-}$ ions do not directly exchange oxygen isotopes with $H_2O$ or $OH^-$, and $CO_3^{2-}$ and $HCO_3^-$ come to $^{18}O$ equilibrium very rapidly relative to the timescale of our interest here. Therefore Eqs. (A-16) and (A-17) can be combined to give a new expression for the rate of change in the $^{18}O$ content of the sum of $H_2CO_3$, $HCO_3^-$ and $CO_3^{2-}$:

$$\frac{d^{18}O([H_2CO_3]+[HCO_3^-]+[CO_3^{2-}])}{dt} = k_{+2}[CO_2](2\alpha+\beta-3\gamma)+k_{+4}[CO_2][OH^-](2\alpha+\theta-3\varepsilon) \quad \text{(A-18a)}$$

By defining $\mu$ as the atom fraction of $^{18}O$ isotopes in $CO_3^{2-}$, the left-hand side of the equation above can be written as:

$$\frac{d(3[H_2CO_3]\gamma+3[HCO_3^-]\varepsilon+3[CO_3^{2-}]\mu)}{dt} = k_{+2}[CO_2](2\alpha+\beta-3\gamma)+k_{+4}[CO_2][OH^-](2\alpha+\theta-3\varepsilon) \quad \text{(A-18b)}$$

In order to simplify the following algebraic manipulations, we assume $\gamma = \varepsilon = \mu$. The fidelity of this assumption was tested by numerically solving the following differential equations (see below) by adopting two boundary conditions; $\gamma = \varepsilon = \mu$ and $\gamma \neq \varepsilon \neq \mu$. For the latter case, the numeric values for $\gamma$, $\varepsilon$ and $\mu$ were assigned according the equilibrium oxygen fractionation factors between individual DIC species and $H_2O$ from Beck et al. (2005). Irrespective of the boundary conditions, however, the final outcomes of the computations were essentially identical. Hence assuming $\gamma = \varepsilon = \mu$, the equation above can be transformed into:

$$3S\cdot\frac{d\gamma}{dt} = k_{+2}[CO_2](2\alpha+\beta-3\gamma)+k_{+4}[CO_2][OH^-]\times(2\alpha+\theta-3\varepsilon) \quad \text{(A-19)}$$

where

$$S = [H_2CO_3]+[HCO_3^-]+[CO_3^{2-}] \quad \text{(A-20)}$$

From Eqs. (A-15) and (A-19), a set of homogeneous differential equations with respect to $\alpha$ and $\gamma$ can be obtained:

$$\frac{d\alpha}{dt} = P(\gamma-\alpha)$$
$$\frac{d\gamma}{dt} = \frac{2}{3}Q\alpha - Q\gamma \quad \text{(A-21)}$$

where

$$P = k_{+2}+k_{+4}[OH^-]$$
$$Q = \frac{k_{+2}[CO_2]+k_{+4}[CO_2][OH^-]}{S} \quad \text{(A-22)}$$

The differential equations (Eq. A-21) have a general solution of the form:

$$\alpha = a_1e^{-\lambda_1 t}+a_2e^{-\lambda_2 t}$$
$$\gamma = b_1e^{-\lambda_1 t}+b_2e^{-\lambda_2 t} \quad \text{(A-23)}$$

where $a_{1,2}$ and $b_{1,2}$ are constants. The differential equations can be solved by arranging a 2 by 2 matrix in this case, such that:

$$\begin{bmatrix}\frac{d\alpha}{dt}\\ \frac{d\gamma}{dt}\end{bmatrix} = \begin{bmatrix}-P & P\\ \frac{2}{3}Q & -Q\end{bmatrix}\begin{bmatrix}\alpha\\ \gamma\end{bmatrix} \quad \text{(A-24)}$$

The eigenvalues $\lambda$ in Eq. (A-23) must satisfy the following relationship:

$$\det.\begin{vmatrix}-(P+\lambda) & P\\ \frac{2}{3}Q & -(Q+\lambda)\end{vmatrix} = 0 \quad \text{(A-25)}$$

The expression above can be simplified to:

$$\lambda^2+(P+Q)\lambda+\frac{1}{3}PQ = 0 \quad \text{(A-26a)}$$

Thus, the solutions ($\lambda_{1,2}$) to the equation are:

$$\lambda_1 = \frac{-(P+Q)+\sqrt{(P+Q)^2-\frac{4}{3}PQ}}{2}$$

and

$$\lambda_2 = \frac{-(P+Q)-\sqrt{(P+Q)^2-\frac{4}{3}PQ}}{2} \quad \text{(A-26b)}$$

From the definition of P and Q (Eq. A-22), the final expressions for $\lambda_1$ and $\lambda_2$ are:

$$\lambda_{1,2} = 0.5(k_{+2}+k_{+4}[OH^-])\left[1+\frac{CO_2}{S}\pm\sqrt{1+\frac{2}{3}\cdot\frac{[CO_2]}{S}+\left(\frac{[CO_2]}{S}\right)^2}\right] \quad \text{(A-27)}$$

The contribution of the term containing $\lambda_1$ to the overall solution (Eq. A-23) is negligible on the timescale concerned here. In other words, the solution can be solely described by the term containing $\lambda_2$, which is identical to the time constant $\tau^{-1}$ in the formulation by Usdowski et al. (1991).

## APPENDIX B. SUPPLEMENTARY DATA

Supplementary data (Tables S1–S12) associated with this article can be found, in the online version, at http://dx.doi.org/10.1016/j.gca.2012.07.022.

## REFERENCES


Adkins J. F., Boyle E. A., Curry W. B. and Lutringer A. (2003) Stable isotopes in deep-sea corals and a new mechanism for "vital effects". *Geochim. Cosmochim. Acta* **67**, 1129–1143.

Al-Horani F. A., Al-Moghrabi S. M. and de Beer D. (2003) Microsensor study of photosynthesis and calcification in the scleractinian coral, *Galaxea fascicularis*: Active internal carbon cycle. *J. Exp. Mar. Biol. Ecol.* **288**, 1–15.

Allison N., Tudhope A. W. and Fallick A. (1996) Factors influencing the stable carbon and oxygen isotopic composition of *Porites lutea* coral skeletons from Phuket, South Thailand. *Coral Reefs* **15**, 43–57.

Beck W. C., Grossman E. L. and Morse J. W. (2005) Experimental studies of oxygen isotope fractionation in the carbonic acid system at 15°, 25° and 40 °C. *Geochim. Cosmochim. Acta* **69**, 3493–3503.

Bentov S., Brownlee C. and Erez J. (2009) The role of seawater endocytosis in the biomineralization process in calcareous foraminifera. *Proc. Natl. Acad. Sci. USA* **106**, 21500–21504.

Bertucci A., Innocenti A., Zoccola D., Scozzafava A., Allemand D., Tambutté S. and Supuran C. T. (2009) Carbonic anhydrase inhibitors: Inhibition studies of a coral secretory isoform with inorganic anions. *Bioorg. Med. Chem. Lett.* **19**, 650–653.

Bertucci A., Zoccola D., Tambutté S., Vullo D. and Supuran C. T. (2010) Carbonic anhydrase activators. The first activation study of a coral secretory isoform with amino acids and amines. *Bioorg. Med. Chem.* **18**, 2300–2303.

Bertucci A., Tambutté S., Supuran C. T., Allemand D. and Zoccola D. (2011) A new coral carbonic anhydrase in *Stylophora pistillata*. *Mar. Biotechnol.* **13**, 992–1002.

Boyer P. D. (1959) Uses and limitations of measurements of rates of isotopic exchange and incorporation in catalyzed reactions. *Arch. Biochem. Biophys.* **82**, 387–409.

Clark A. M. and Perrin D. D. (1951) A re-investigation of the question of activators of carbonic anhydrase. *Biochem. J.* **48**, 495–503.

Coplen T. B., Kendall C. and Hopple J. (1983) Comparison of stable isotope reference samples. *Nature* **302**, 236–238.

Corrège T., Delcroix T., Rècy J., Beck W., Cabioch G. and Cornec F. L. (2000) Evidence for stronger El Niño-Southern Oscillation (ENSO) events in a mid-Holocene massive coral. *Paleoceanography* **15**, 465–470.

de Nooijer L. J., Toyofuku T. and Kitazato H. (2009) Foraminifera promote calcification by elevating their intracellular pH. *Proc. Natl. Acad. Sci. USA* **106**, 15374–15378.

DeVoe H. and Kistiakowsky G. B. (1960) The enzymatic kinetics of carbonic anhydrase from bovine and human erythrocytes. *J. Am. Chem. Soc.* **83**, 274–280.

Dodgson S. J., Gros G., Krawiec J. A., Lin L., Bitterman N. and Forster R. E. (1990) Comparison of $^{18}O$ exchange and pH stopflow assays for carbonic anhydrase. *J. Appl. Physiol.* **68**, 2443–2450.

Donaldson T. L. and Quinn J. A. (1974) Kinetic constants determined from membrane transport measurements: Carbonic anhydrase activity at high concentrations. *Proc. Natl. Acad. Sci. USA* **71**, 4995–4999.

Erez J. (2003) The source of ions for biomineralization in foraminifera and their implications for paleoceanographic proxies. *Rev. Mineral. Geochem.* **54**, 115–149.

Felis T., Pätzold J. and Loya Y. (2003) Mean oxygen-isotope signatures in *Porites* spp. corals: Inter-colony variability and correction for extension-rate effects. *Coral Reefs* **22**, 328–336.

Furla P., Galgani I., Durand S. and Allemand D. (2000) Sources and mechanisms of inorganic carbon transport for coral calcification and photosynthesis. *J. Exp. Biol.* **203**, 3445–3457.

Gao Y. Q. and Marcus R. A. (2001) Strange and unconventional isotope effects in ozone formation. *Science* **293**, 259–263.

Ghannam A. F., Tsen W. and Rowlett R. S. (1986) Activation parameters for the carbonic anhydrase II-catalyzed hydration of $CO_2$. *J. Biol. Chem.* **261**, 1164–1169.

Harned H. S. and Davis R. J. (1943) The ionization constant of carbonic acid in water and the solubility of carbon dioxide in water and aqueous salt solutions from 0 to 50 °C. *J. Am. Chem. Soc.* **65**, 2030–2037.

Harned H. S. and Owen B. B. (1958) *The Physical Chemistry of Electrolytic Solutions*. Reinhold, New York.

Harned H. S. and Scholes S. R. J. (1941) The ionization constant of $HCO_3^-$ from 0 to 50 °C. *J. Am. Chem. Soc.* **63**, 1706–1709.

Higbie J. (1991) Uncertainty in the linear regression slope. *Am. J. Phys.* **59**, 184–185.

Ip Y. K., Lim A. L. L. and Lim R. W. L. (1991) Some properties of calcium-activated adenosine triphosphate from the hermatypic coral *Galaxea fascicularis*. *Mar. Biol.* **111**, 191–197.

Jørgensen B. B., Erez J., Revsbech N. P. and Cohen Y. (1985) Symbiotic photosynthesis in a planktonic foraminiferan, *Globigerinoides sacculifer* (Brady), studied with microelectrodes. *Limnol. Oceanogr.* **30**, 1253–1267.

Juillet-Leclerc A., Reynaud S., Rollion-Bard C., Cuif J. P., Dauphin Y., Blamart D., Ferrier-Pagès and Allemand D. (2009) Oxygen isotope signature of the skeletal microstructures in cultured corals: Identification of vital effects. *Geochim. Cosmochim. Acta* **73**, 5320–5332.

Keith M. L. and Webber J. N. (1965) Systematic relationship between carbon and oxygen isotopes in carbonates deposited by modern corals and algae. *Science* **150**, 498–501.

Kernohan J. C. (1965) The pH-activity curve of bovine carbonic anhydrase and its relationship to the inhibition of the enzyme by anions. *Biochim. Biophys. Acta* **96**, 304–317.

Kim S.-T., Mucci A. and Taylor B. E. (2007) Phosphoric acid fractionation factors for calcite and aragonite between 25 and 75 °C: Revisited. *Chem. Geol.* **246**, 135–146.

Köhler-Rink S. and Kühl M. (2005) The chemical microenvironment of the symbiotic planktonic foraminifer *Orbulina universa*. *Mar. Biol. Res.* **1**, 68–78.

Lea D. W., Bijma J., Spero J. and Archer D. (1999) Implications of a carbonate ion effect on shell carbon and oxygen isotopes for glacial ocean conditions. In *Use of Proxies in Paleoceanography: Examples From the South Atlantic* (eds. G. Fischer and G. Wefer). Springer, Berlin, pp. 512–522.

Lindskog S. (1960) Purification and properties of bovine erythrocyte carbonic anhydrase. *Biochim. Biophys. Acta* **39**, 218–226.

Mackenzie F. T. and Lerman A. (2006) *Carbon in the Geobiosphere – Earth's Outer Shell*. Springer, Netherlands, pp. 89–122.

Maier C., Felis T., Pätzold J. and Bak R. P. M. (2004) Effects of skeletal growth and lack of species effects in the skeletal oxygen isotope climate signal within the coral genus *Porites*. *Mar. Geol.* **207**, 193–208.

McConnaughey T. (1989a) $^{13}C$ and $^{18}O$ isotopic disequilibrium in biological carbonates: I. Patterns. *Geochim. Cosmochim. Acta* **53**, 151–162.

McConnaughey T. (1989b) $^{13}C$ and $^{18}O$ isotopic disequilibrium in biological carbonates: II. *In vitro* simulation of kinetic isotope effects. *Geochim. Cosmochim. Acta* **53**, 163–171.

McConnaughey T. (2003) Sub-equilibrium oxygen-18 and carbon-13 levels in biological carbonates: Carbonate and kinetic models. *Coral Reefs* **22**, 316–327.

McCrea J. M. (1950) On the isotopic chemistry of carbonates and a paleotemperature scale. *J. Chem. Phys.* **18**, 849–857.

Mills G. A. and Urey H. C. (1940) The kinetics of isotopic exchange between carbon dioxide, bicarbonate ion, carbonate ion and water. *J. Am. Chem. Soc.* **62**, 1019–1026.

Miyamoto H., Miyashita T., Okushima M., Nakano S., Morita T. and Matsushiro A. (1996) A carbonic anhydrase from the nacreous layer in oyster pearls. *Proc. Natl. Acad. Sci.* **93**, 9657–9960.

Moya A., Tambutté S., Bertucci A., Tambutté E., Lotto S., Vullo D., Supuran C. T., Allemand D. and Zoccola D. (2008) Carbonic anhydrase in the scleractinian coral *Stylophora pistillata*: Characterization, localization, and role in biomineralization. *J. Biol. Chem.* **283**, 25475–25484.

Nimer N., Guan Q. and Merrett M. J. (1994) Extra- and intracellular carbonic anhydrase in relation to culture age in a high-calcifying stain of *Emiliania huxleyi* Lohman. *New Phytol.* **126**, 601–607.

Omata T., Suzuki A., Sato T., Minoshima K., Nomaru E., Murakami A., Murayama S., Kawahata H. and Maruyama T. (2008) Effect of photosynthetic light dosage on carbon isotope composition in the coral skeleton: Long-term culture of *Porites* spp. *J. Geophys. Res.* **113**, G02014. http://dx.doi.org/10.1029/2007JG000431.

Paneth P. and O'Leary M. H. (1985) Carbon isotope effect on dehydration of bicarbonate ion catalyzed by carbonic anhydrase. *Biochemistry* **24**, 5143–5147.

Pinsent B. R. W., Pearson L. and Roughton F. J. W. (1956) The kinetics of combination of carbon dioxide with hydroxide ions. *Trans. Faraday Soc.* **52**, 2930–2934.

Pocker Y. and Bjorkquist D. W. (1977) Comparative studies of bovine carbonic anhydrase in $H_2O$ and $D_2O$. Stopped-flow studies of the kinetics of interconversion of $CO_2$ and $HCO_3^-$. *Biochemistry* **16**, 5698–5707.

Rink S., Kühl M., Bijma J. and Spero H. J. (1998) Microsensor studies of photosynthesis and respiration in the symbiotic foraminifer *Orbulina universa*. *Mar. Biol.* **131**, 583–595.

Rollion-Bard C. and Erez J. (2010) Intra-shell boron isotope rations in the symbiont-bearing benthic foraminiferan *Amphistegina lobifera*: Implications for $\delta^{11}B$ vital effects and paleo-pH reconstructions. *Geochim. Cosmochim. Acta* **74**, 1530–1536.

Rollion-Bard C., Chaussidon M. and France-Lanord C. (2003) pH control on oxygen isotopic composition of symbiotic corals. *Earth Planet. Sci. Lett.* **215**, 275–288.

Rollion-Bard C., Erez J. and Zilberman T. (2008) Intra-shell oxygen isotope ratios in the benthic foraminifera genus *Amphistegina* and the influence of seawater carbonate chemistry and temperature on this ratio. *Geochim. Cosmochim. Acta* **72**, 6006–6014.

Rollion-Bard C., Blamart D., Cuif J. P. and Dauphin Y. (2010) In situ measurements of oxygen isotopic composition in deep-sea coral, *Lophelia pertusa*: Re-examination of the current geochemical models of biomineralization. *Geochim. Cosmochim. Acta* **74**, 1338–1349.

Rollion-Bard C., Chaussidon M. and France-Lanord C. (2011) Biological control of internal pH in scleractinian corals: Implications on paleo-pH and pale-temperature reconstructions. *C. R. Geoscience* **343**, 397–405.

Rosenfeld M., Yam R., Shemesh A. and Loya Y. (2003) Implication of water depth on stable isotope composition and skeletal density banding patterns in a *Porites lutea* colony: Results from a long-term translocation experiments. *Coral Reefs* **22**, 337–345.

Rost B., Riebesell U., Burkhardt S. and Sültemeyer D. (2003) Carbon acquisition of bloom-forming marine phytoplankton. *Limnol. Oceanogr.* **48**, 55–67.

Roughton F. J. W. (1941) The kinetics and rapid thermochemistry of carbonic acid. *J. Am. Chem. Soc.* **63**, 2930–2934.

Shackleton N. J. and Kennett N. J. (1975) Paleotemperature history of the Cenozoic and the initiation of Antarctic glaciations: Oxygen and carbon isotope analyses in DSDP sites 277, 279, and 281. *Init. Rep. Deep Sea Drill. Proj.* **29**, 743–755.

Silverman D. N. (1973) Carbonic anhydrase catalyzed oxygen-18 exchange between bicarbonate and water. *Arch. Biochem. Biophys.* **155**, 452–457.

Soto A. R., Zheng H., Shoemaker D., Rodriguez J., Read B. A. and Wahlund A. (2006) Identification and preliminary characterization of two cDNAs encoding unique carbonic anhydrases from the marine alga *Emiliania huxleyi*. *Appl. Environ. Microbiol.* **72**, 5500–5511.

Spero H. J., Bijma J., Lea D. W. and Bemis B. E. (1997) Effect of seawater carbonate concentration on foraminiferal carbon and oxygen isotopes. *Nature* **390**, 497–500.

Steiner H., Jonsson B.-H. and Lindskog S. (1975) The catalytic mechanism of carbonic anhydrase: Hydrogen-isotope effects on the kinetic parameters of the human C isoenzyme. *Eur. J. Biochem.* **59**, 253–259.

Tambutté S., Tambutté E., Zoccola D., Caminiti N., Lotto S., Moya A., Allemand D. and Adkins J. (2006) Characterization and role of carbonic anhydrase in the calcification process of the azooxanthellate coral *Tubastrea aurea*. *Mar. Biol.* **151**, 71–83.

Tambutté S., Holcomb M., Ferrier-Pagès C., Reynaud S., Tambutté É., Zoccola D. and Allemand D. (2011) Coral biomineralization: From gene to the environment. *J. Exp. Mar. Biol. Ecol.* **408**, 58–78.

ter Kuile B., Erez J. and Padan E. (1989) Competition for inorganic carbon between photosynthesis and calcification in the symbiont-bearing foraminifer *Amphistegina lobifera*. *Mar. Biol.* **103**, 253–259.

Thode H. G., Shima M., Rees C. E. and Krishnamurty K. V. (1965) Carbon-13 isotope effects in systems containing carbon dioxide, bicarbonate, carbonate and metal ions. *Can. J. Chem.* **43**, 582–595.

Tudhope A. W., Chilcott C. P., McCulloch M. T., Cook E. R., Chappell J., Ellam R. M., Lea D. W., Lough J. M. and Shimmield G. B. (2001) Variability in the El Niño-Southern Oscillation through a glacial-interglacial cycle. *Science* **291**, 1511–1517.

Uchikawa J. and Zeebe R. E. (2010) Examining possible effects of seawater pH decline on foraminiferal stable isotopes during the Paleocene–Eocene Thermal Maximum. *Paleoceanography* **25**, PA2216. http://dx.doi.org/10.1029/2009PA001864.

Usdowski E. and Hoefs J. (1993) Oxygen isotope exchange between carbonic acid, bicarbonate, carbonate, and water: A re-examination of the data of McCrea (1950) and an expression for the overall partitioning of oxygen isotopes between the carbonate species and water. *Geochim. Cosmochim. Acta* **57**, 3815–3818.

Usdowski E., Michaelis J., Böttcher M. E. and Hoefs J. (1991) Factors for the oxygen isotope equilibrium fractionation between aqueous and gaseous $CO_2$, carbonic acid, bicarbonate, carbonate, and water (19 °C). *Z. Phys. Chem.* **170**, 237–249.

Wang X., Conway W., Burns R., McCann N. and Maeder M. (2010) Comprehensive study of the hydration and dehydration reactions of carbon dioxide in aqueous solution. *J. Phys. Chem. A* **114**, 1734–1740.

Wilbur K. M. and Anderson N. G. (1948) Electrometric and colorimetric determination of carbonic anhydrase. *J. Biol. Chem.* **176**, 147–154.

Worthington V. (1993) *Worthington Enzyme Manual*. Worthington Biomedical Corporation, Lakewood, New Jersey.

Yu Z., Xie L., Lee S. and Zhang R. (2006) A novel carbonic anhydrase from the mantle of the pearl oyster (*Pinctada fucata*). *Comp. Biochem. Phys. B* **143**, 190–194.

Zachos J., Pagani M., Sloan J., Thomas E. and Billups K. (2001) Trends, rhythms, and aberrations in global climate 65Ma to present. *Science* **292**, 686–693.

Zeebe R. E. (1999) An explanation of the effect of seawater carbonate concentration on foraminiferal oxygen isotopes. *Geochim. Cosmochim. Acta* **63**, 2001–2007.

Zeebe R. E. (2001) Seawater pH and isotopic paleotemperatures of Cretaceous oceans. *Palaeogeogr. Palaeoclimatol. Palaeoecol.* **170**, 49–57.

Zeebe R. E. (2007) An expression for the overall oxygen isotope fractionation between the sum of dissolved inorganic carbon and water. *Geochem. Geophys. Geosyst.* **8**, Q09002. http://dx.doi.org/10.1029/2007GC001663.

Zeebe R. E. and Sanyal A. (2002) Comparison of two potential strategies of planktonic foraminifera for house building: $Mg^{2+}$ or $H^+$ removal? *Geochim. Cosmochim. Acta* **66**, 1159–1169.

Zeebe R. E. and Wolf-Gladrow D. (2001) $CO_2$ in Seawater: Equilibrium, Kinetics Isotopes. vol. 65. Elsevier Oceanography Series, Elsevier, Amsterdam.

*Associate editor:* Claire Rollion-Bard